

PROJECT REPORT

on

**Phase Change Material-Based Cooling for Electric
Vehicle Battery Packs**

Completed by
Aditya Chaudhary

Under the Guidance of
Dr. Mahesh Kumar Yadav,
Ph.D. (IIT Kanpur, India)



**Department of Mechanical Engineering
Punjab Engineering College (Deemed to be University)
Chandigarh**

NOVEMBER 2025

ABSTRACT

The adoption of electric vehicles (EVs) is accelerating worldwide due to their environmental benefits, reduced running costs, and advancements in battery technology. Global EV sales reached 17 million units in 2024, capturing 20% of total car sales—a milestone achievement. With projections of 20-22 million units and 24-25% market share in 2025, the electric vehicle revolution is accelerating rapidly. This growth is supported by unprecedented government and industry commitments, including Europe's €172 billion infrastructure investment and a global charging market projected to reach \$121-164 billion by 2030. With this surge in usage, there is a growing need to address operational challenges that impact performance and longevity.

One critical issue is battery overheating, especially during extended operation or in hot climates where ambient temperatures can exceed 40°C. High temperatures can degrade battery performance by up to 20%, reduce energy efficiency, and shorten lifespan by as much as 30%. In severe cases, overheating poses safety risks such as thermal runaway. Traditional cooling methods typically include air cooling, where fans or ducts channel ambient air over the battery pack, and liquid cooling, which circulates coolant through channels or plates in contact with battery cells. Air cooling is simple and inexpensive but often inadequate in high-demand or high-temperature situations. Liquid cooling provides better heat transfer (up to 3–5 times more effective than air cooling) but adds weight, increases the cost, and overall system complexity. Even with these systems, maintaining consistent, safe operating temperatures in all driving conditions remains a challenge.

In the present study, the patented serpentine cooling pipe technology from the Tesla Model S battery cooling system is taken as a reference and plan to integrate Phase Change Material (PCM) into it to improve the thermal performance. The goal is to develop a modified cooling system that combines both liquid and PCM cooling design to make a cost effective and efficient model.

The work flow is to study and analyse the cooling system design of the Tesla Model S, investigate the integration of Phase Change Materials (PCM) for hot climate applications, and simulate a hybrid battery thermal management system. The study will focus on the selection of suitable PCM, its effective integration into the existing cooling architecture, and the evaluation of the overall thermal performance of the modified system. The proposed concept will be examined and validated through simulations using Ansys software. Moreover, a small scale working physical prototype of hybrid PCM model will also be made

By merging established cooling technology with PCM-based enhancements, this research aims to address the specific thermal management needs of the Indian EV market. The expected outcome is a cost-effective, high-performance solution that can extend battery life, improve efficiency, and maintain safety standards under extreme temperature conditions.

TABLE OF CONTENT

ABSTRACT	ii
TABLE OF CONTENT	iii
TABLE OF FIGURES	iv
INTRODUCTION	1
LITERATURE REVIEW	2
PROBLEM IDENTIFICATION	4
METHODOLOGY	7
WORK FLOW	8
ALTERNATE METHODS	9
ASSESSMENT OF COOLING DESIGNS	10
SELECTING OPTIMUM PCM	17
HYBRID PCM AND WATERN COOLING MODEL	18
CAD MODEL	18
MESHING AND DOMAIN DEFINING	21
PHYSICS AND BOUNDARY SETUP	24
SOLVER SETUP	24
PCM SIMULATION RESULTS	25
COMPARITIVE ANALYSIS	26
CELL BOUNDARY TEMPERATURE	26
TEMPERATURE AT OUTLET	28

COST ESTIMATION	29
PHYSICAL PROTOTYPE	30
Mechanical Structure and Cooling Channel Fabrication	30
Battery Configuration and Load Simulation	30
Temperature Measurement Setup	30
PCM Integration	31
Hybrid Cooling Demonstration	31
CONCLUSION	33
FUTURE SCOPE	34
REFRENCES	35

TABLE OF FIGURE

Figure 1: Variation of Battery SOH with time at different climate condition (<i>Charlotte Argue 2024</i>)	4
Figure 2: Variation of Battery SOH with time at different usage (<i>Charlotte Argue 2024</i>)	5
Figure 3: Variation of Cell Temperature with Time with or without PCM (<i>Shankar Dhurgam 2021</i>)	5
Figure 4: Variation of Temperature with Time (Guo, C. Y., 2025)	6
Figure 5: Classification of battery cooling methods	10
Figure 6: 2D view of inlet(65mmX5mm)	11
Figure 7 :2D sketch of serpentine pattern	11
Figure 8 :3D Serpentine pattern after sweeping	11
Figure 9: Isometric View of CAD model	11
Figure 10: Solid model of an 18650-size cylindrical cell ($\varnothing 18 \text{ mm} \times 65 \text{ mm}$)	11

Figure 11: Top view of battery module	12
Figure 12: Front view of the battery module	12
Figure 13: mesh of liquid cooling system	13
Figure 14: Meshing config	14
Figure 15: Meshing config	14
Figure 16: close up of meshed image	14
Figure 17: meshing config of different domain	14
Figure 18:Temperature contour of the battery module	16
Figure 19: Temperature distribution on cell body	16
Figure 20: Iteration of liquid cooling	17
Figure 21: CAD model of PCM design	19
Figure 22:CAD model of cells and copper pipes	20
Figure 23: Cad model without aluminium cover	20
Figure 24: Meshing table of different domain	22
Figure 25: Meshed up image of CAD model	22
Figure 26: Close up image of mesh	23
Figure 27: Meshing settings	23
Figure 28: meshing setting	23
Figure 29: Temperature Contour of PCM model	25
Figure 30: Iteration graph of PCM model	26
Figure 31: Graph indicating PCM is melting	26
Figure 32: Cell Boundary Temperature of PCM model	27
Figure 33: Cell boundary temperature of liquid cooling model	27
Figure 34: Temp at outlet of liquid cooling model	28
Figure 35: Temp at outlet of PCM model	29

Figure 36: 18650 Cells	31
Figure 37: Copper pipes	31
Figure 38: Cell and tube setup	32
Figure 39: Temperature Sensor	32
Figure 40: Paraffin Wax	32
Figure 41: Final Model	33

INTRODUCTION

Electric vehicles (EVs) are seeing rapid adoption worldwide, including in India, due to growing awareness of environmental concerns, reduction in running costs, and advances in battery technology. However, operating conditions especially in regions like northern India where ambient summer temperatures regularly exceed 45°C present specific challenges for battery thermal management. Literature suggests that elevated cell temperatures accelerate degradation rates compared to moderate conditions, leading to reduced efficiency and lifespan. For example, after 200 charge cycles, capacity loss is around 6.7% at 45 °C, compared to 3.3% at 25 °C (Thawkar & Dhoble, 2023; Kang et al., 2023).

Existing EV cooling systems, such as air and liquid cooling designs, have proven effective in some climates but each comes with certain limitations air cooling is simpler and lighter but often inadequate in extreme heat, while liquid cooling improves performance but adds weight, complexity, and cost. International manufacturers use methods like serpentine pattern (Tesla) and Top cooling method (BYD) However, adaptation of such systems for Indian summer extremes is less explored.

This project takes a research-based approach to evaluate how phase change material (PCM) integration can improve temperature control in EV battery packs. Instead of assuming benefits, our work will use simulations to examine how PCM can buffer peak temperature spikes under realistic Indian driving and parking conditions. The PCM layer will be modelled to absorb heat during short high-load events, with its placement, volume, and melting temperature assessed against ambient conditions and cooling airflow.

For the current study, SolidWorks and ANSYS 24 Academic were used as the primary tools for geometry creation, meshing, simulation, and post-processing. SolidWorks was employed for developing the 3D CAD model of the battery module. The assembled geometry was then exported in STEP format and imported into ANSYS Design Modeler for defining the fluid domain of inside the serpentine pattern. ANSYS Meshing and Fluent modules within the ANSYS 24 Academic suite were utilized for generating the computational mesh, applying boundary conditions, and performing steady-state CFD analysis to evaluate the thermal performance of the system.

Then we moved into the material study. We reviewed different classes of PCM organic, inorganic, and eutectic to see which one could realistically handle the thermal swings expected in Indian summers. After comparing melting ranges, thermal stability, cycling durability, and safety, RT44 emerged as the most practical fit for our module because its phase-change temperature aligns well with the operating EV cells.

With that selection made, we integrated RT44 into the battery-module model and ran a new set of simulations using the same workflow as liquid cooling model. The results were clear: the PCM layer consistently damped temperature spikes and kept the module closer to its ideal operating band, especially under high-load and high-ambient scenarios.

LITERATURE REVIEW

Ahmadian-Elmi, M., & Zhao, P. (2024)

This paper provides a comprehensive review of thermal management strategies for cylindrical lithium-ion battery packs, emphasizing performance, safety, and lifespan enhancement. The authors analyze four major approaches: air cooling, liquid cooling, phase change material (PCM) cooling, and hybrid systems, comparing their heat dissipation efficiency, temperature uniformity, and cost-effectiveness. Air cooling is found simple but less efficient for high-power applications, while liquid cooling offers superior uniformity with added complexity. PCM and hybrid methods show strong potential for passive or combined cooling. The study concludes that hybrid systems leveraging both active and passive methods deliver optimal thermal control for cylindrical battery modules. Ahmadian-Elmi and Zhao's findings provide an essential foundation for developing efficient, compact, and sustainable battery thermal management systems supporting future EV battery pack innovations integrating liquid and PCM-based hybrid cooling.

Gharehghani et al. (2024)

This paper, published in Renewable and Sustainable Energy Reviews, provides an extensive review of modern Battery Thermal Management Systems (BTMS) for electric vehicles, emphasizing performance, safety, and sustainability. The study discusses active, passive, and hybrid cooling methods, highlighting the growing importance of Phase Change Materials (PCM) in improving thermal uniformity and managing transient heat loads. It explains that while liquid cooling offers high efficiency, integrating PCM enhances passive heat absorption and stabilizes temperature fluctuations, making hybrid PCM–liquid systems highly effective for high-capacity Li-ion batteries. The paper also explores challenges such as thermal runaway, battery aging, and the role of BTMS in fast-charging safety. Insights from this study guided our project's approach, where we adopted PCM-based thermal regulation integrated with a serpentine liquid-cooling layout to leverage the latent heat storage of PCM for better temperature control under high ambient and transient operating conditions.

GreyB Research Team (2025)

This paper focuses on AI-based thermal management systems for EV batteries. The research shows that machine learning models can predict temperature behaviour and help control cooling systems automatically. The study explains that using AI with sensor data helps improve the efficiency of battery cooling while reducing power consumption. GreyB's findings suggest that smart control systems are important in future EV designs where passive cooling alone may not be enough.

Talha, M., Singh, R., & Patel, A. (2025)

RSC (2025) discusses hybrid strategies that combine PCM and Hybrid Energy Storage Systems (HESS) to reduce chances of thermal runaway in EV batteries. The paper states that only PCM is sometimes not enough when temperature increases too fast. But combining it with other systems like forced air flow or intelligent control gives better safety. It also talks about how paraffin-based PCM is commonly used because it is stable, safe, and stores large amount of heat without pressure risk.

Thawkar, P., & Dhoble, A. (2023)

Thawkar, P., & Dhoble, A. (2023). review different battery thermal management systems (BTMS) for electric vehicles and point out the limitations of traditional cooling methods. They find that air-based cooling systems are simple and cheap but not so effective for high heat conditions. Liquid cooling improves performance but comes with higher cost and complexity. The study highlights how Phase Change Material (PCM) can act as a passive cooling method by absorbing excess heat during its melting process. The authors argue that PCM is safer and energy-efficient and can be used with other cooling systems for better results.

Kang, X., Li, Y., Wu, D., & Zhang, Q. (2023)

This study explores the thermal performance of paraffin-based PCM in EV battery packs. The research conducts simulation-based tests to see how well PCM can maintain temperature under different heat loads. Results show that PCM helps delay the rise in battery temperature and keeps it in a safe range during high usage. The paper also mentions that PCM placement and geometry of the duct are important for better heat transfer. This study supports the idea that PCM is effective for peak heat absorption in EVs.

Patil et al. (2023)

This paper focuses on optimizing liquid-cooled battery thermal management systems at the module level for electric vehicles. Using CFD and multi-objective optimization (HEEDS), the study compares original and Z-type cooling plates to enhance temperature uniformity and reduce pressure drop. Results show a 22% improvement in temperature difference and a 24% reduction in pressure loss. However, the study assumes steady-state conditions and does not include transient or PCM effects.

PROBLEM IDENTIFICATION

Electric vehicle (EV) batteries generate significant heat during charging, discharging, and extended use in hot weather. According to the U.S. Department of Energy, lithium-ion batteries operate best between 15 °C and 35 °C, and prolonged exposure above 40 °C can accelerate annual capacity loss by up to 20%. Fast charging alone can produce as much as 2.5 kW of heat in a typical 150 kW session, and if this heat is not properly dissipated, temperatures can climb beyond 45 °C, forcing the battery management system to throttle performance. Studies published by the National Renewable Energy Laboratory (NREL) show that high operating temperatures can shorten battery life by 30–50% and, above ~60–70 °C, can trigger thermal runaway—a chain reaction that can damage or destroy the pack.

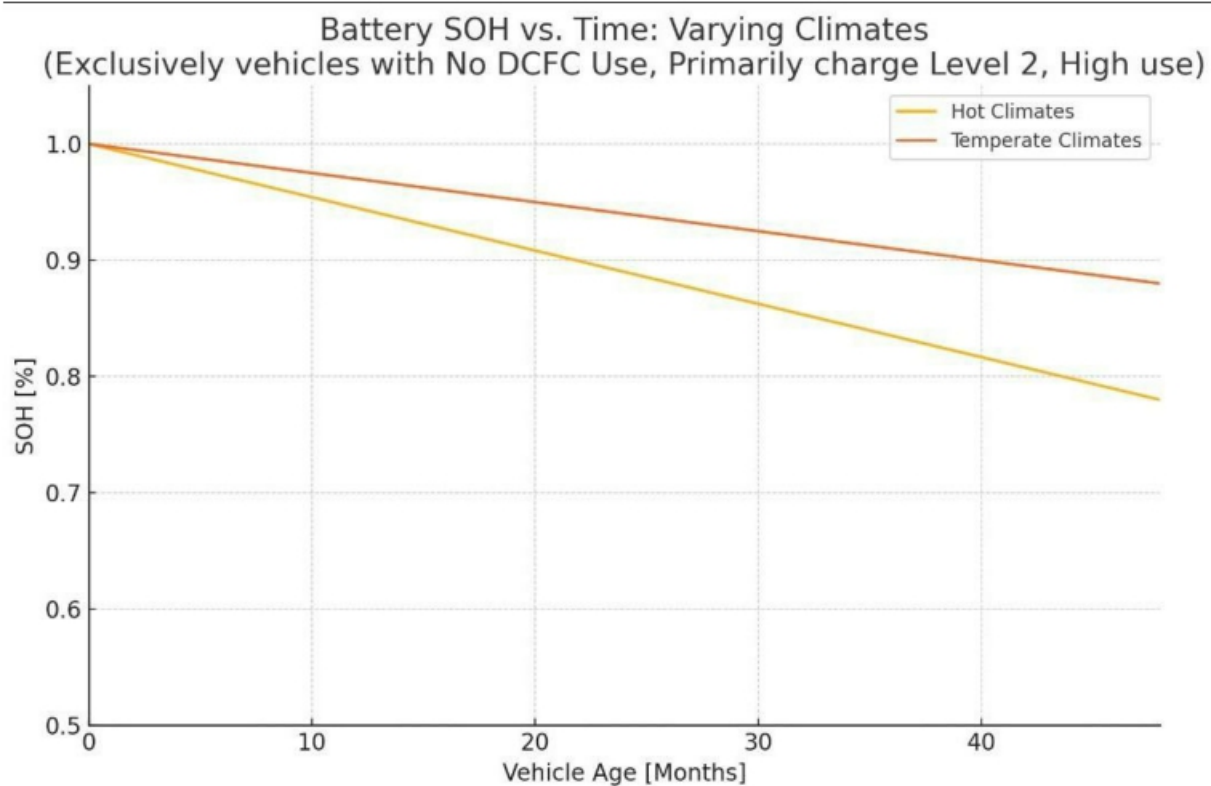


Figure 1: Variation of Battery SOH with time at different climate condition (*Charlotte Argue 2024*)

In the context of Indian summers, this heat challenge becomes more severe. While typical EV batteries in moderate climates lose about 1.8% of capacity per year, India's summer heat often pushes degradation rates higher, especially when packs run hot or remain parked in direct sunlight. Lithium-ion cells perform best below ~35 °C; above this threshold, chemical aging accelerates sharply. Laboratory tests have shown that storing a battery for one year at 45 °C can result in ~7% capacity loss, compared to only ~1% at 25 °C. Cycling at 45–65 °C further increases degradation compared to ~23 °C. In practice, liquid-cooled EVs in India may limit loss to ~2–4% annually, but repeated hot-soak parking, frequent DC fast charging, or exposure to heat waves can push loss well above temperate averages.

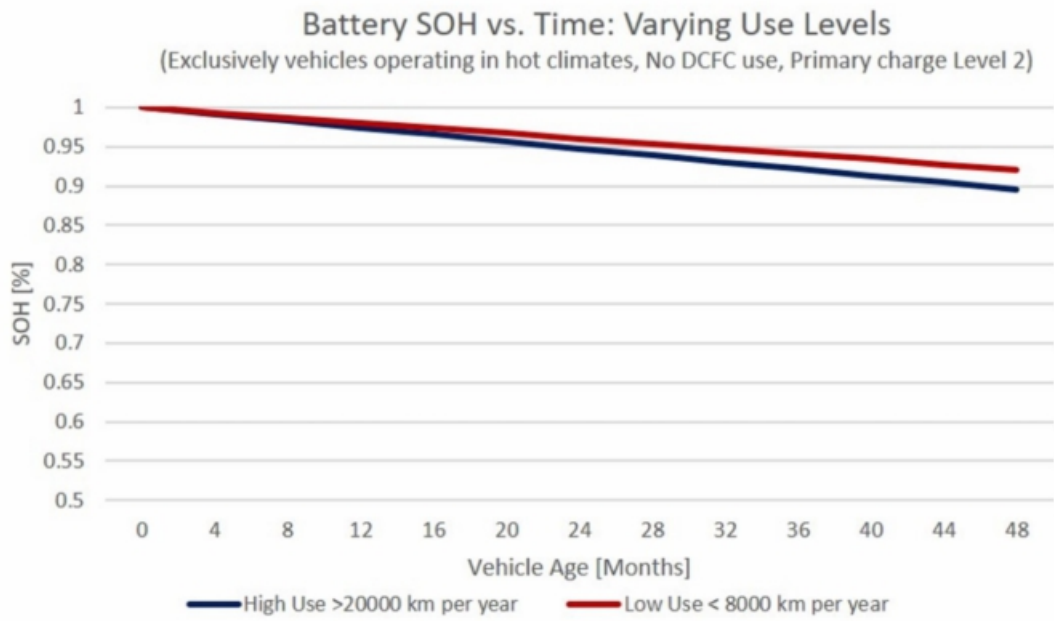


Figure 2: Variation of Battery SOH with time at different usage (Charlotte Argue 2024)

Heat affects not only long-term degradation but also short-term efficiency. On hot days, real-world datasets show minimal range loss at 32 °C (<5%), but once ambient temperatures exceed 38 °C (100 °F), range can drop by 17–18%, largely due to HVAC and battery cooling loads. Over time, these losses add up. For example, a battery starting at 100% state of health and losing 3% per year would retain ~91–92% capacity after three years and ~85–88% after five years under careful management, while persistent high-heat use could lower these figures further.

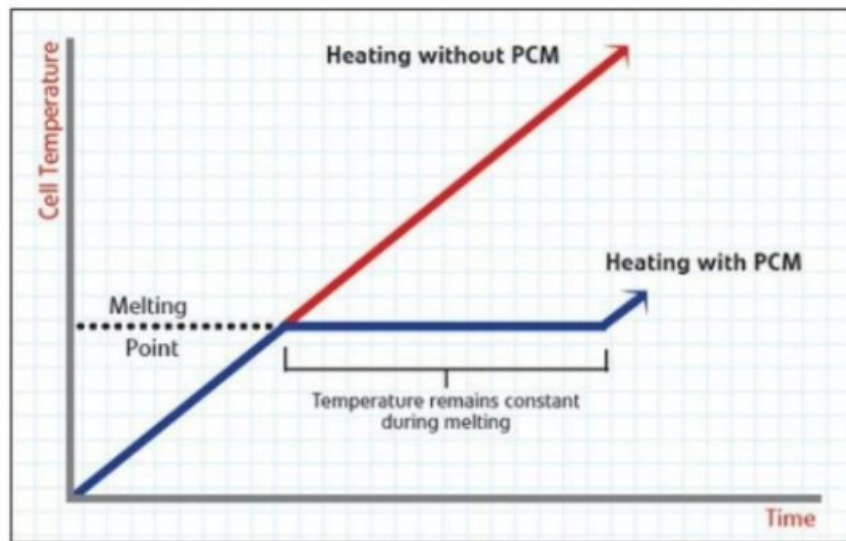


Figure 3: Variation of Cell Temperature with Time with or without PCM (Shankar Dhurgam 2021)

Traditional cooling approaches—air cooling and liquid cooling—each have drawbacks. Air cooling is simple and cost-effective but often insufficient in severe heat, while liquid cooling improves temperature control but adds weight, cost, and system complexity. Passive cooling using Phase

Change Material (PCM) offers a potential middle ground. PCM absorbs heat during its melting phase, holding battery temperature near its melting point and delaying further rise. This can smooth out temperature spikes and reduce cooling system load.

When integrated with PCM, it can be deployed adaptively cooling more during short-term heat spikes and conserving energy when conditions are stable. For prolonged heat exposure, supplemental cooling may still be needed. Tests have shown that combining PCM with airflow management reduces battery temperature rise by about 8–12 °C compared to airflow alone, especially in high-load conditions.

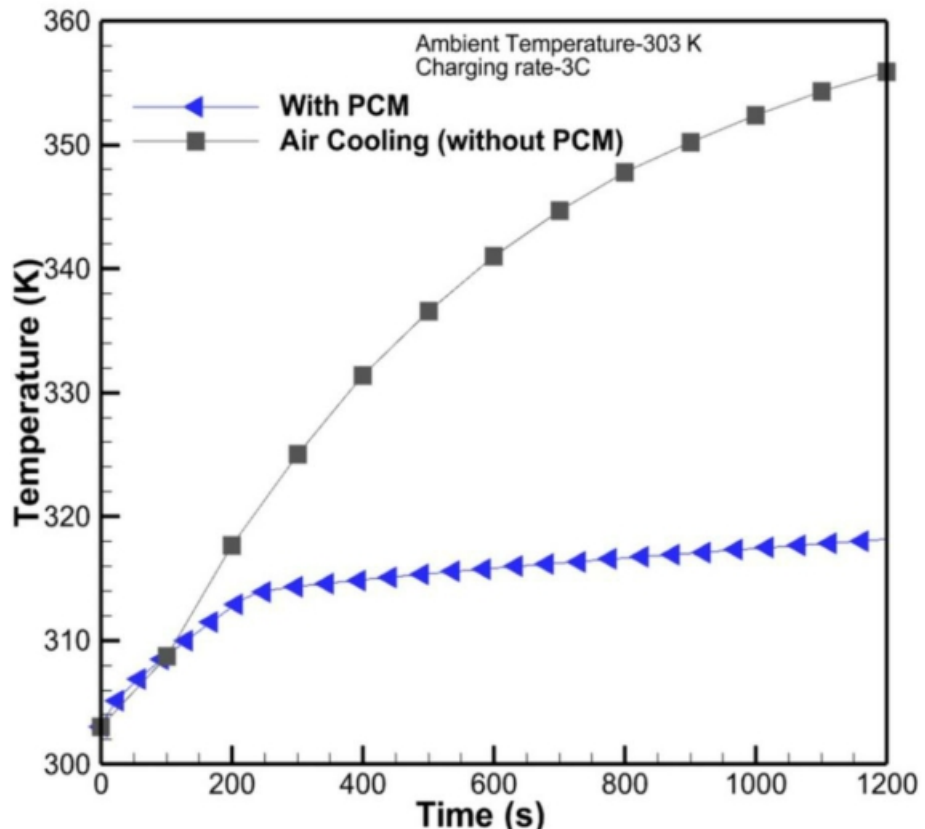


Figure 4: Variation of Temperature with Time (Guo, C. Y., 2025)

This approach could be particularly valuable for EVs in India, where high summer temperatures coincide with growing EV adoption. By pairing the simplicity of air cooling with the thermal stability of PCM, it is intended to extend battery life, improve safety, and maintain performance all without redesigning the battery pack or adding excessive cost

METHODOLOGY

The methodology chosen for this project is Computational Fluid Dynamics (CFD) simulation using ANSYS Fluent. This approach allows detailed analysis of the thermal and flow characteristics within the battery array and its cooling systems under varying operating conditions. The study aims to evaluate and compare the thermal performance of liquid cooling and PCM-based cooling for Li-Ion battery arrays at small scale.

The methodology follows a systematic workflow adapted from the reference study on water cooling, with extensions made for PCM integration and comparative analysis.

WORK FLOW

1. Literature Review

We began by reviewing existing research on Li-ion battery thermal management, with a focus on liquid-cooling systems and PCM-based hybrid cooling approaches. Studies covering CFD modelling, water-cooled serpentine channels, and PCM phase-change behaviour were examined to understand current design practices, limitations, and validated numerical models.

2. Liquid-Cooling System Development

2.1 CAD Model Preparation

A baseline liquid-cooled battery module was modelled using CAD tools. The geometry was designed to match the reference serpentine water-cooling study to allow validation. This included the battery cell array and coolant aluminium channel

2.2 Import and Design Completion

The CAD assembly was exported in STEP format and imported into ANSYS DesignModeler. The fluid domain inside the serpentine channel and solid and fluid regions were defined for conjugate heat-transfer analysis.

2.3 Mesh Generation and Domain Defining

A high-quality mesh was generated with refinement near battery surfaces and narrow coolant passages. Mesh independence tests were performed to ensure stable results and minimal sensitivity to further refinement. Various named selections were made like inlet, outlet and cell boundary to define the contact regions and boundary conditions

2.4 Physics and Boundary Setup

The next step was defining material properties, coolant behaviour, turbulence model, and conjugate heat-transfer interfaces. Boundary conditions such as inlet temperature, flow rate, ambient temperature, and temperature at cell interface were applied.

2.5 Solver Setup and Liquid-Cooling Solution

A transient solver with second-order discretization was used to capture time-dependent temperature rise during discharge. Simulations were run to validate the model and match trends from the reference study.

3. PCM-Based Cooling Study

3.1 PCM Selection and Material Study

Based on the literature survey, different PCM types were evaluated. RT44 was selected because its melting range aligns with EV cell operating temperatures in Indian conditions.

3.2 PCM Model CAD Development

A new version of the battery module was created with an integrated PCM layer. The geometry maintained the same cell arrangement to allow direct comparison with the liquid-cooling model.

3.3 Mesh Generation for PCM Model

A refined mesh was created for both the solid cell region and the PCM block. Special attention was given to capturing heat conduction paths and phase-change zones.

3.4 Physics and Boundary Setup for PCM

The enthalpy porosity method was used to model PCM melting and solidification. Heat generation, ambient conditions, and thermal interfaces were set to match the liquid-cooling configuration for fair comparison.

3.5 Solver Setup and PCM Solution

Transient simulations were run to evaluate melting fraction, heat-absorption capacity, and temperature evolution under realistic high-ambient scenarios.

4. Comparative Analysis

Results from the validated liquid-cooling model and the PCM model were compared using different parameters. This helped quantify the advantage of PCM in buffering temperature spikes and slowing heat buildup.

5. Prototype Fabrication (PCM Concept)

A small PCM-integrated demonstration prototype was prepared to visualize the concept and show how the material can be incorporated around a battery module. This model is only for demonstration purposes and not intended for performance testing.

6. Documentation and Reporting

All steps including assumptions, geometry details, mesh statistics, solver settings, simulation results, comparison plots, and conclusions—were compiled into a comprehensive project report.

ALTERNATE METHODS

Air Cooling uses airflow around battery modules to remove heat through convection. It is simple, low-cost, and works for entry-level EVs in mild climates. But air has low heat transfer capability, causing uneven temperatures, making it unsuitable for fast charging or high-performance vehicles.

Liquid Cooling circulates a water-glycol coolant through channels or plates attached to batteries. It provides 100–1000× better heat transfer than air, ensures ±2–5°C uniformity, supports 150–270 kW fast charging, and operates in wide climates (−20°C to +50°C). It is the industry standard used in 65–75% of EVs, including long-range passenger cars, commercial fleets, delivery vehicles, and premium EVs. It slightly increases cost and weight but greatly improves battery health and range.

PCM Cooling uses phase-change materials that absorb heat during the solid-to-liquid transition. It requires no energy, provides excellent short-term temperature control, and helps prevent thermal runaway. However, PCM cannot continuously remove heat and is therefore used only as a supporting

passive system together with liquid or air cooling to reduce peak temperature swings and improve temperature uniformity.

Hybrid Cooling combines multiple cooling approaches such as air–liquid, liquid–PCM, or air–PCM to utilize the strengths of both active and passive methods. In these systems, liquid cooling manages continuous heat removal, PCM absorbs sudden high-power spikes, and airflow helps cool areas not directly in contact with coolant plates. By integrating these mechanisms, hybrid systems achieve better temperature uniformity, lower maximum cell temperatures, improved efficiency, and more stable performance than any single method alone, making them suitable for modern EV packs operating under varied load and environmental conditions.

Although liquid cooling is known for its strong heat transfer and support for fast charging, newer hybrid systems that combine phase change materials (PCM) with liquid cooling are rapidly advancing, offering higher efficiency and lighter designs.

ASSESSMENT OF COOLING DESIGNS

Cold Plate Cooling uses stamped or machined aluminum plates with coolant channels touching battery modules. It offers good manufacturability and low cost for mainstream EVs, supporting standard charging and daily driving needs.

Micro-channel Cooling integrates many small parallel channels inside plates to boost surface area and create turbulent flow. This improves heat transfer 2–5× over standard cold plates. It is preferred in premium EVs and high-rate fast charging where performance is critical.

Direct Contact Serpentine Ribbon — The Best Solution

Direct Contact Serpentine Ribbon Cooling places long, curved coolant tubes directly between cylindrical cells. This eliminates thermal resistance, ensures <3–5°C temperature difference, and maintains cell temperatures <40°C even during fast charging and high-power output. Aluminum ribbons with multiple internal micro-channels maximize heat transfer while keeping pumping power low. Manufacturing via extrusion + bending makes it cost-effective and lightweight (only 1.5–2.5 kg per module). This technology is proven in Tesla vehicles and considered the optimal choice for next generation high-energy cylindrical cell EVs.

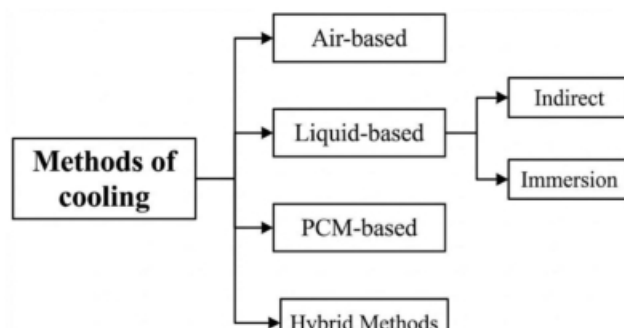


Figure 5: Classification of battery cooling methods

LIQUID COOLING RIBBON COOLING MODEL

CAD MODEL

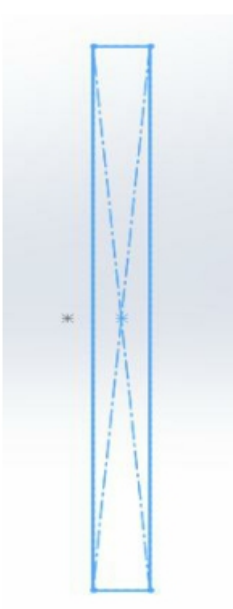


Figure 6:2D view of inlet(65mmX5mm)

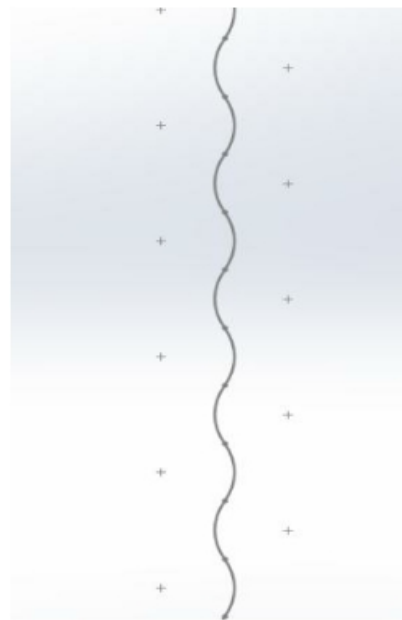


Figure 7 :2D sketch of serpentine pattern

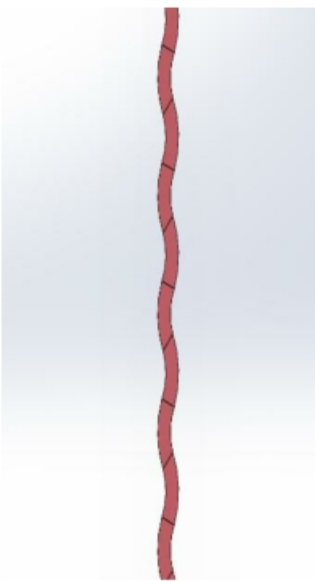


Figure 8 :3D Serpentine pattern after sweeping

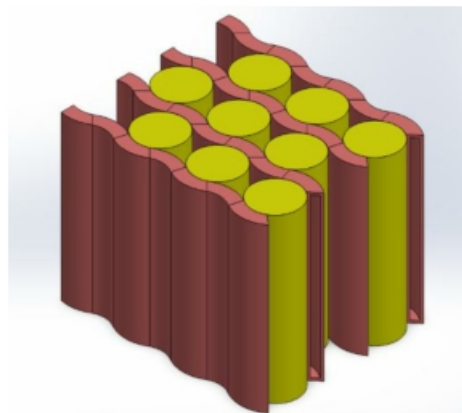


Figure 9: Isometric View of CAD model

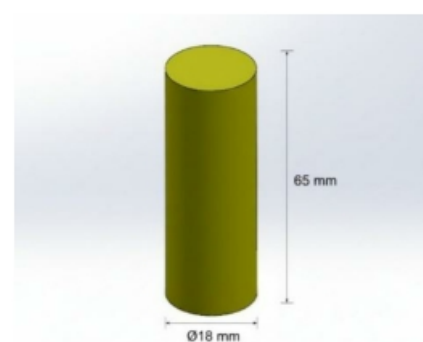


Figure 10: Solid model of an 18650-size cylindrical cell ($\varnothing 18$ mm \times 65 mm)

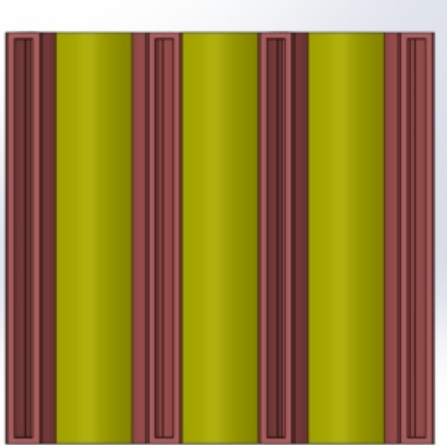


Figure 12: Front view of the battery module

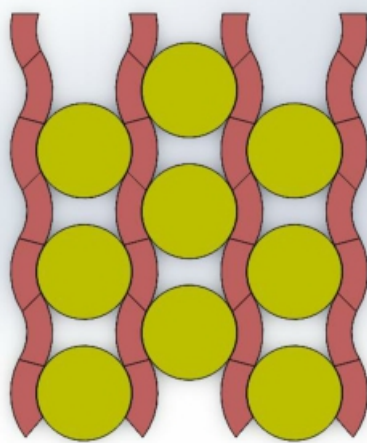


Figure 11: Top view of battery module

The CAD model of the Li-Ion battery array with an integrated liquid cooling system was developed using SolidWorks and ANSYS Design Modular. The process began in SolidWorks, where the serpentine cooling channel was designed. A 2D sketch of the serpentine pattern was created, and the sweep feature was applied to generate the 3D cooling path. The channel was modelled with a thin cross-section to represent the coolant passage, allowing effective heat transfer and realistic fluid flow conditions.

Inlet and outlet ports were incorporated to define the coolant entry and exit points. The serpentine layout was optimized to ensure uniform flow distribution across the battery surfaces while maintaining compactness suitable for electric vehicle integration.

The geometry of the Li-Ion cells was then modelled and assembled with the serpentine cooling structure to create a complete battery array model. The design aimed to replicate the configuration described in the reference study, providing a realistic representation of an EV battery pack with liquid cooling integration.

After finalizing the geometry, the assembly was exported as a STEP file and imported into ANSYS Design Modular. Using the capping feature, the fluid domain was defined within the serpentine channels, representing the coolant volume. This ensured that both solid and fluid regions were accurately captured for CFD analysis.

The finalized CAD model represented the small-scale liquid cooling system, closely following the methodology and configuration of the reference paper. This model served as the foundation for meshing, boundary condition setup, and subsequent CFD simulations in ANSYS Fluent.

ANSYS MESHING AND DOMAIN DEFINING

The meshing process was carried out in ANSYS Meshing to discretize the geometry of the Li-Ion battery array along with the integrated liquid cooling system. Since the model included narrow serpentine channels and curved surfaces, tetrahedral elements were used throughout to accurately capture the geometry and ensure smooth representation of complex regions within the fluid domain.

A curvature-based size function was applied to refine the mesh in areas with high geometric variation and expected thermal gradients. Local refinement was introduced near the cooling channel walls and the interfaces between the coolant and battery surfaces to improve prediction accuracy for both temperature and flow fields. Mesh quality checks were performed to verify skewness, aspect ratio, and element quality, ensuring stable and accurate simulation results.

The final mesh provided a good balance between precision and computational efficiency, allowing for steady-state simulations to converge smoothly. All quality metrics were found to be within acceptable limits, confirming that the mesh was suitable for CFD analysis.

The final mesh consisted of 566,140 nodes and 475,011 triangular elements, which effectively resolved both the solid and fluid domains while maintaining a manageable computational load.

After completing the mesh, the computational domains were defined to prepare the model for boundary condition assignment. Individual regions were identified for the coolant inlet, coolant outlet, the fluid passages within the serpentine channels, the solid battery cells, and the channel casing. Defining these domains at this stage is important because it allows each part of the model to receive the correct physical conditions such as flow and temperature inputs at the inlet, pressure at the outlet, internal heat generation within the cells, and no-slip walls along the channel surfaces. Proper domain separation also ensures accurate conjugate heat transfer between the solid and fluid regions, which is essential for capturing realistic temperature distributions in the final CFD solution.

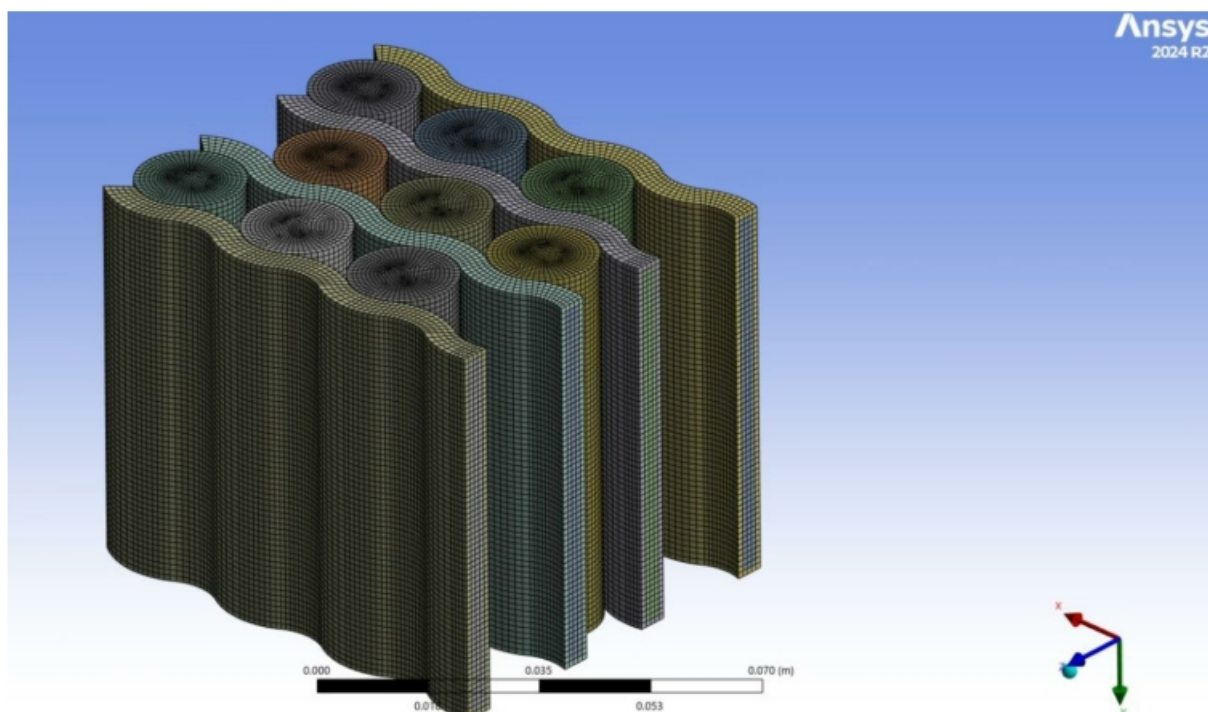


Figure 13: mesh of liquid cooling system

Details of "Mesh"	
Physics Preference	CFD
Solver Preference	Fluent
<input type="checkbox"/> Element Size	5.e-002 m
Export Format	Standard
Export Preview Surface Mesh	No
Sizing	
Use Adaptive Sizing	No
<input type="checkbox"/> Growth Rate	Default (1.2)
<input type="checkbox"/> Max Size	Default (0.1 m)
Mesh Defeaturing	Yes
<input type="checkbox"/> Defeature Size	Default (2.5e-004 m)
Capture Curvature	Yes
<input type="checkbox"/> Curvature Min Size	Default (5.e-004 m)
<input type="checkbox"/> Curvature Normal Angle	Default (18.0°)
Capture Proximity	No
Bounding Box Diagonal	0.12804 m
Average Surface Area	1.0589e-003 m ²
Minimum Edge Length	5.1051e-003 m

Figure 14: Meshing config

<input type="checkbox"/> Growth Rate	Default (1.2)
<input type="checkbox"/> Max Size	Default (2.e-003 m)
Mesh Defeaturing	Yes
<input type="checkbox"/> Defeature Size	Default (5.e-006 m)
Capture Curvature	Yes
<input type="checkbox"/> Curvature Min Size	Default (1.e-005 m)
<input type="checkbox"/> Curvature Normal Angle	Default (18.0°)
Capture Proximity	No
Bounding Box Diagonal	0.12397 m
Average Surface Area	3.66e-004 m ²
Minimum Edge Length	2.7764e-004 m
Quality	
Inflation	
Advanced	
Statistics	
<input type="checkbox"/> Nodes	566140
<input type="checkbox"/> Elements	475011
Show Detailed Statistics	No

Figure 15: Meshing config

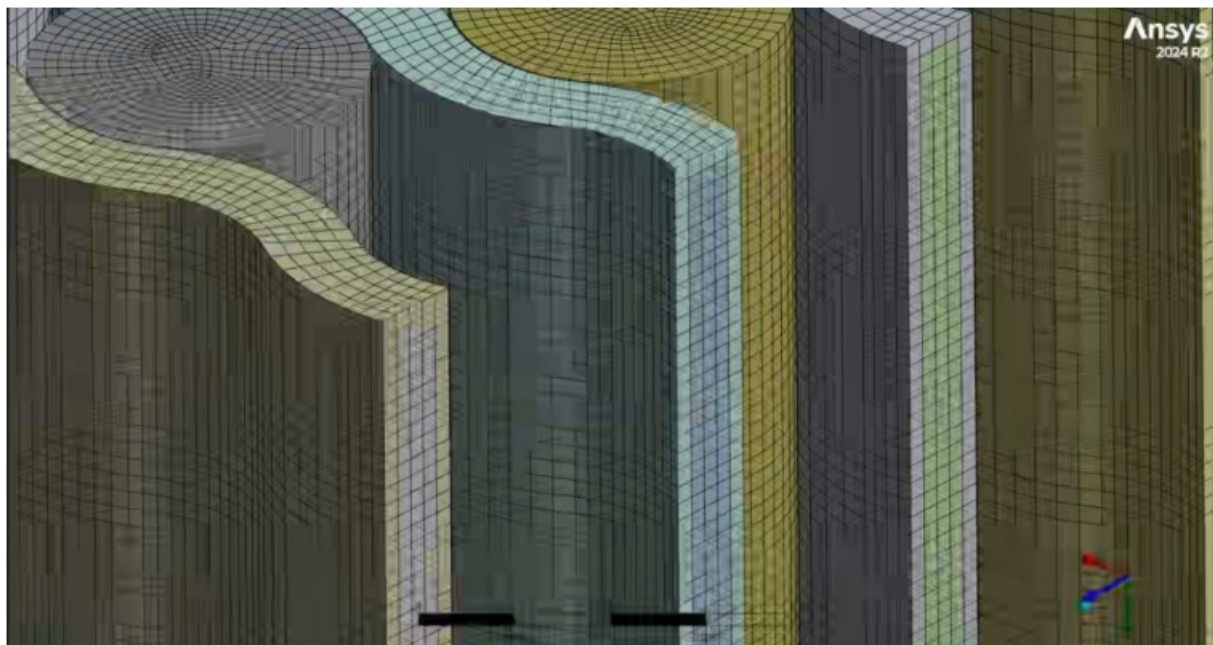


Figure 16: close up of meshed image

Domain	Nodes	Elements
cells cell	382140	361985
channel	90304	44608
fluid	23040	16821
fluid fluid.1	23808	17388
fluid fluid.2	23040	16821
fluid fluid.3	23808	17388
All Domains	566140	475011

Figure 17: meshing config of different domain

PHYSICS AND BOUNDARY SETUP

The physics setup defined the thermal interaction between the battery cells and the coolant flowing through the serpentine channels. Water was assigned as the working fluid with temperature-dependent properties enabled so that viscosity, density, and thermal conductivity adjusted realistically with temperature. This helped the model capture how the coolant's behaviour changed as it absorbed heat from the cells. The solid battery domains were treated as conjugate regions, allowing heat to conduct through the cell bodies and into the channel surfaces without any artificial insulation at the interfaces. Each cell was maintained at an internal operating temperature of 50 °C, representing steady heat generation during discharge.

Flow turbulence was handled using the k-epsilon model with enhanced wall treatment because the serpentine layout generates secondary flows, curvature effects, and thin near-wall layers that need proper resolution. A velocity inlet of 2 m/s at 23 °C was applied at the coolant entry, while the outlet was defined as a pressure boundary at atmospheric conditions. All channel walls were treated as no-slip and thermally coupled surfaces. Together, these boundary definitions ensured realistic heat exchange, appropriate flow development, and accurate temperature gradients across the entire geometry.

SOLVER SETUP

A transient solver was chosen to capture how the cooling system responded over time rather than jumping directly to a final steady state. The total simulation time of 300 seconds, with a timestep of one second, provided enough temporal resolution to track the early cooling phase and the later stabilisation phase. Second-order discretisation schemes were used for momentum and energy equations to maintain smooth gradients and avoid numerical diffusion, especially in regions where temperature and velocity changed rapidly.

Residual convergence was monitored closely as the solver progressed, and each timestep showed stable behaviour with gradual reduction in continuity, momentum, and turbulence residuals. The energy residual consistently approached the order of 10^{-7} , indicating that the thermal field had fully stabilised before advancing to the next timestep. This level of numerical stability ensured that the predicted cooling behaviour truly represented the physics rather than solver artefacts.

LIQUID COOLING SOLUTION

The cooling system showed an immediate thermal response as the cold water entered the serpentine channels and began extracting heat from the 50 °C cells. The area-weighted temperature plot captured this clearly, showing a steep drop during the first part of the simulation before gradually levelling off. After roughly 300 seconds, the domain settled around 300.55–300.58 K, marking a stable thermal equilibrium between the coolant and the solid regions.

Temperature contours revealed that the lower regions of the cells, positioned closest to the coolant channels, remained noticeably cooler. Slightly higher temperatures appeared near the upper parts of the cells, where direct exposure to the coolant was minimal. Even then, the peak recorded

temperatures stayed around 322–323 K, and most of the module remained in the favourable 310–315 K range. The serpentine orientation increased coolant residence time and encouraged stronger mixing, which prevented localised hot spots and kept thermal gradients smooth across all three rows of cells.

Altogether, the liquid-cooling arrangement produced a well-controlled temperature distribution with no signs of instability or thermal runaway. It demonstrated that the geometrical layout, flow rate, and material selections were effective enough for a compact multi-cell battery module.

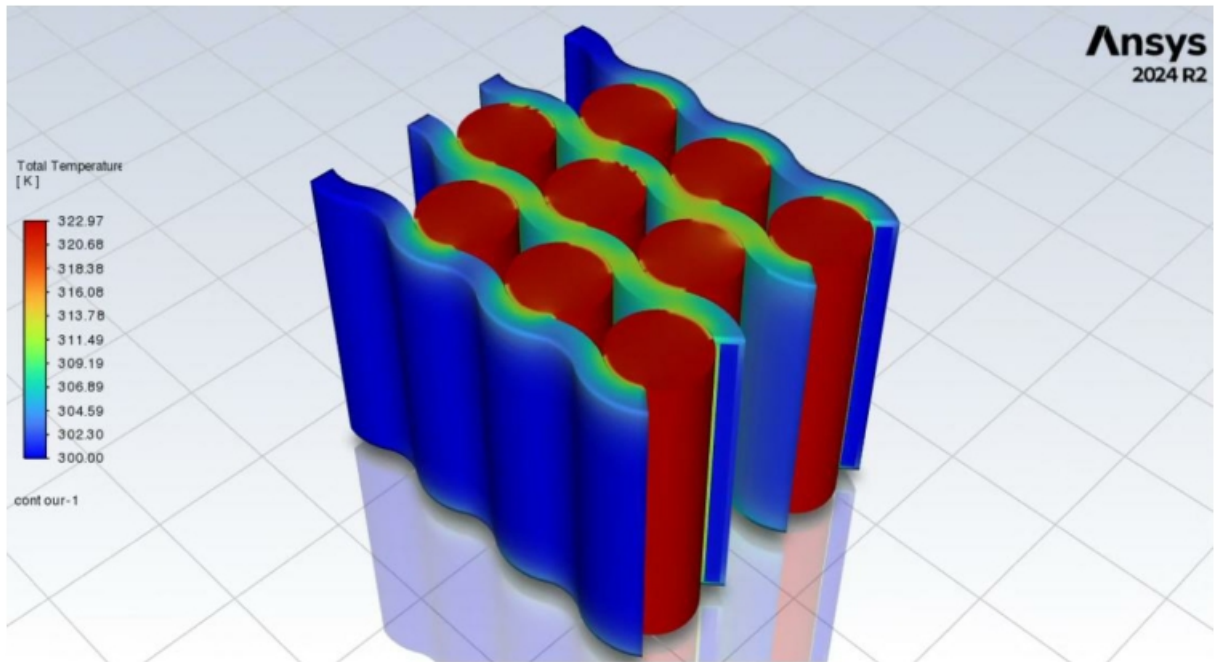


Figure 18: Temperature contour of the battery module

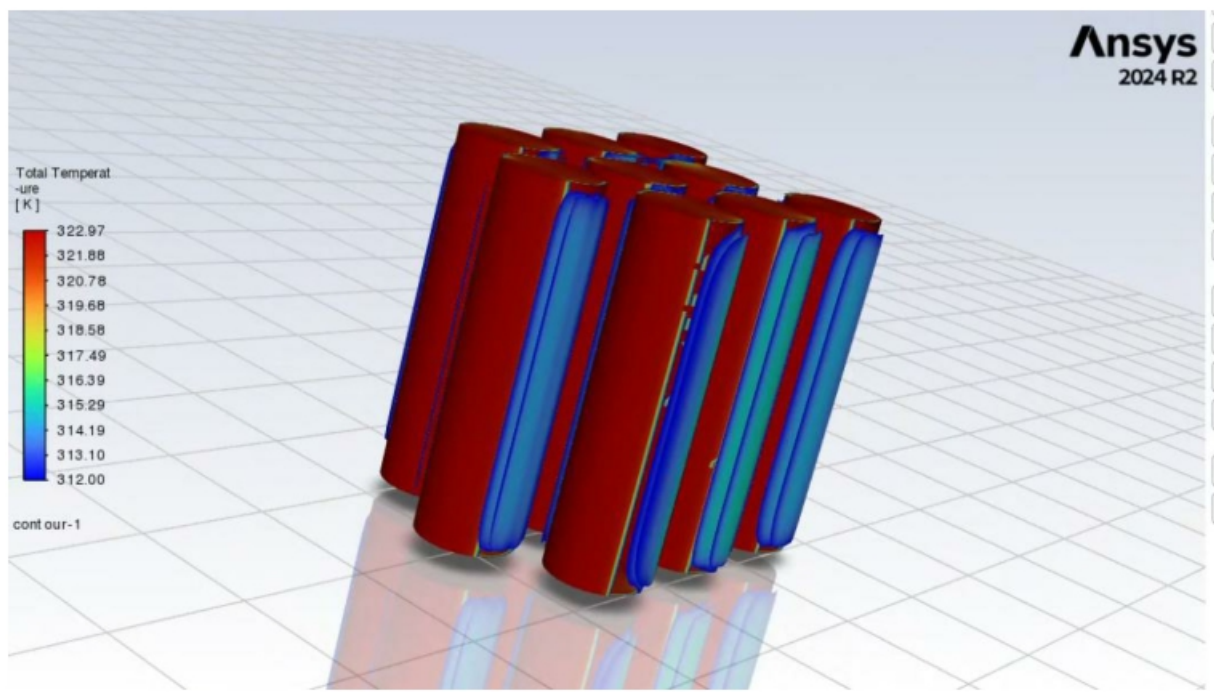


Figure 19: Temperature distribution on cell body

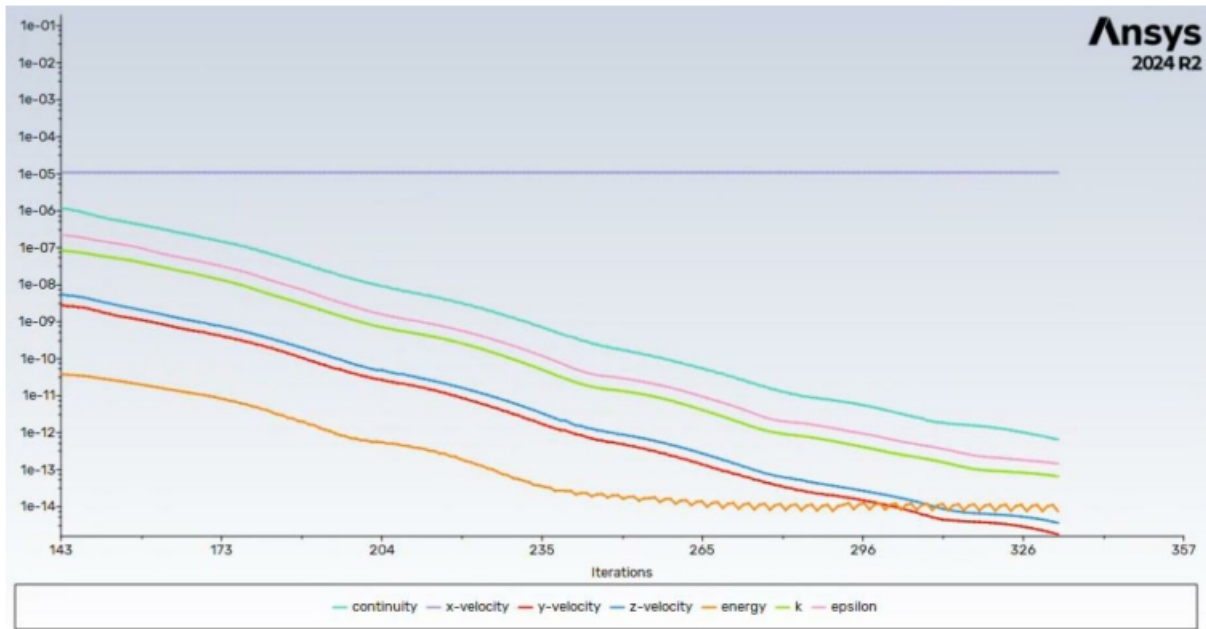


Figure 20: Iteration of liquid cooling

SELECTING OPTIMUM PCM

UNDERSTANDING HOW PCM WORKS

Phase Change Materials acted as passive thermal buffers in our hybrid cooling system by absorbing heat during their solid–liquid transition. When battery temperatures rose above the PCM’s melting point, the material melted and absorbed heat as latent energy, preventing rapid thermal escalation. As temperatures decreased, the PCM solidified and released the stored heat in a controlled manner, stabilizing the temperature profile of the pack. This behavior was particularly effective under Indian operating conditions, where ambient temperatures frequently exceeded 45 °C and imposed sudden thermal stress on lithium-ion cells.

TYPES OF PCM

Organic PCMs offered stable melting temperatures, chemical reliability, non-corrosive behaviour, and good cycling life. Paraffin waxes and fatty acids were widely available in India and provided cost-effective thermal buffering, making them the most suitable category for EV battery systems.

Inorganic PCMs such as hydrated salts provided higher thermal conductivity but suffered from phase segregation, corrosion, and poor long-term stability. These characteristics made them unsuitable for EV battery cooling despite their strong heat storage capability.

Eutectic PCMs delivered sharp melting points and high latent heat performance but were expensive, less available, and demonstrated complex long-term behaviour. As a result, they were more appropriate for premium or experimental vehicles rather than mass-market EVs.

PARAMETERS FOR PCM SELECTION

- Required melting range between 40–45 °C to activate during Indian peak temperatures.
- High latent heat capacity to manage fast charging, acceleration, and hill-climb heat loads.
- Adequate specific heat capacity to store sensible heat before melting.
- Enhanced thermal conductivity, supported through expanded graphite additions.
- Strong cycling durability with no leakage or chemical breakdown across repeated cycles.
- Fully non-corrosive and chemically stable with aluminum components and battery casings.
- Reliable fire safety and encapsulation performance for EV integration.
- Cost suitability for mass-market EVs, supporting overall system affordability.
- Effective integration with our hybrid PCM-and-water cooling design.

SELECTED RT44 PCM AND ITS SUITABILITY

RT44 paraffin-based PCM was selected because it matched the thermal response requirements of Indian EV operation and provided the optimal balance between performance, safety, stability, and cost. Its melting window aligned precisely with the temperature rise observed during high-load conditions, while expanded-graphite enhancement supported rapid heat distribution and effective re-solidification. The material demonstrated strong chemical stability, excellent cycling behaviour, and compatibility with automotive cooling structures. Domestic availability and low raw material cost further strengthened its suitability for scalable EV manufacturing.

KEY REASONS FOR SELECTING RT44 PCM

- Melting range of 41–44 °C activated at exactly the right temperature under Indian climatic loads.
- Maintained battery temperatures in the safe operating zone during peak load events.
- Prevented cell temperatures from exceeding 65 °C, reducing the risk of thermal runaway.
- Expanded-graphite composite improved heat conductivity significantly.
- Low material cost due to full domestic sourcing of paraffin and graphite.
- High cycling stability made it suitable for continuous daily EV operation in hot climates.

HYBRID PCM AND WATER COOLING MODEL

CAD MODEL

The PCM-based cooling model was built with a focus on capturing realistic heat-spreading behaviour inside a compact battery module. The first elements incorporated into the design were the three copper conductors placed at different vertical levels within the enclosure. One wire was positioned

near the base of the module, the second at mid-height, and the third closer to the top. All three ran between the cells. Their purpose was to act as passive heat spreaders, redistributing thermal energy across the PCM volume and reducing localised overheating. Including these wires directly in the CAD model ensured that their conductive influence would be reflected in the subsequent transient phase-change simulations.

With the thermal-spreading structure defined, the nine Li-ion cells were arranged inside the aluminium enclosure in a 3S3P configuration. The cells were positioned with consistent spacing to allow PCM infiltration between them while still maintaining a realistic pack density. The positioning also preserved uniform thermal interaction among the cells, which was important for achieving comparable simulation conditions with the liquid-cooling model. The aluminium housing provided a rigid, thermally conductive boundary, functioning both as a mechanical casing and as an interface for potential external heat rejection.

Once the wiring and cell placement were finalised, the remaining internal volume of the enclosure was defined as the PCM domain. In a practical setting, this corresponds to filling the box with RT44 in molten form so that it surrounds the cells completely before solidifying into a uniform block. Modelling the PCM as a continuous domain allowed accurate representation of heat conduction, melting, and solidification without artificial voids or discontinuities. The geometry was kept clean and meshing-friendly, ensuring that all interfaces: PCM to cells, PCM to copper, and PCM to aluminium are well-defined for correct physics assignment in ANSYS.

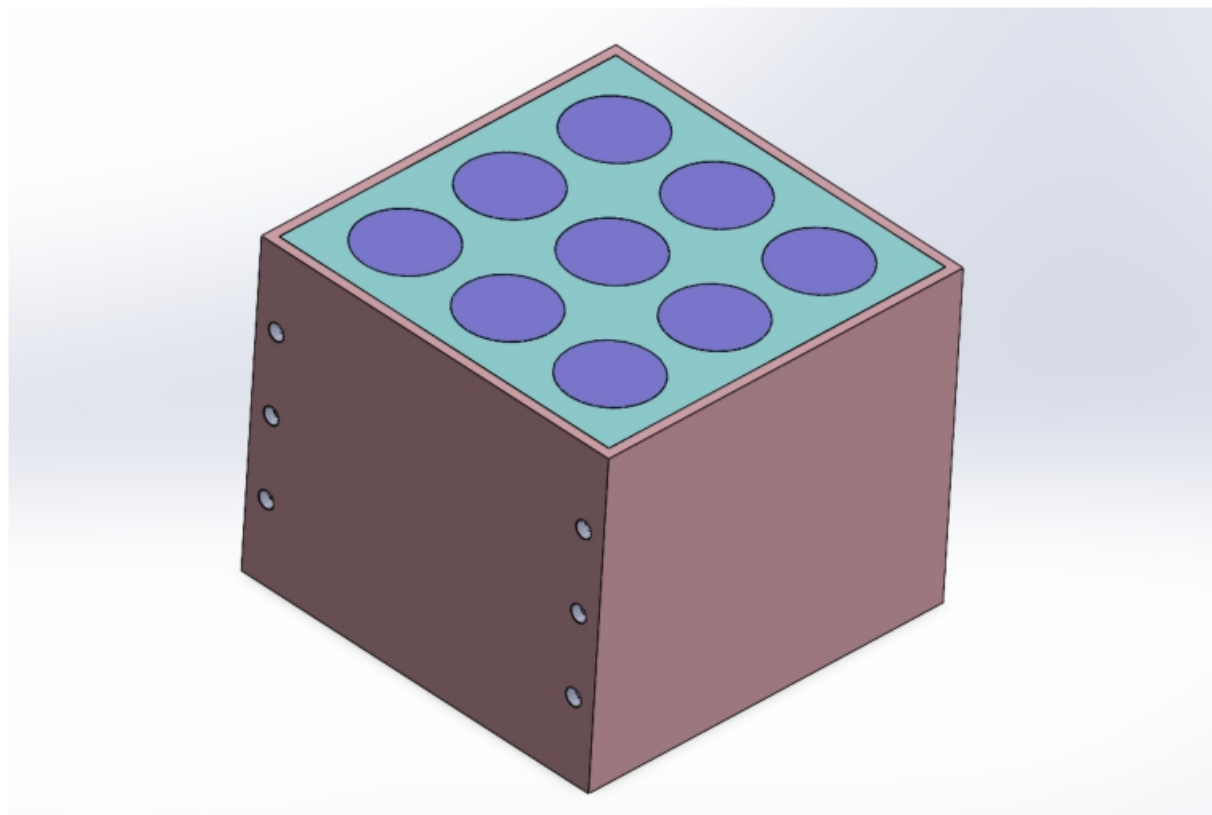


Figure 21: CAD model of PCM design

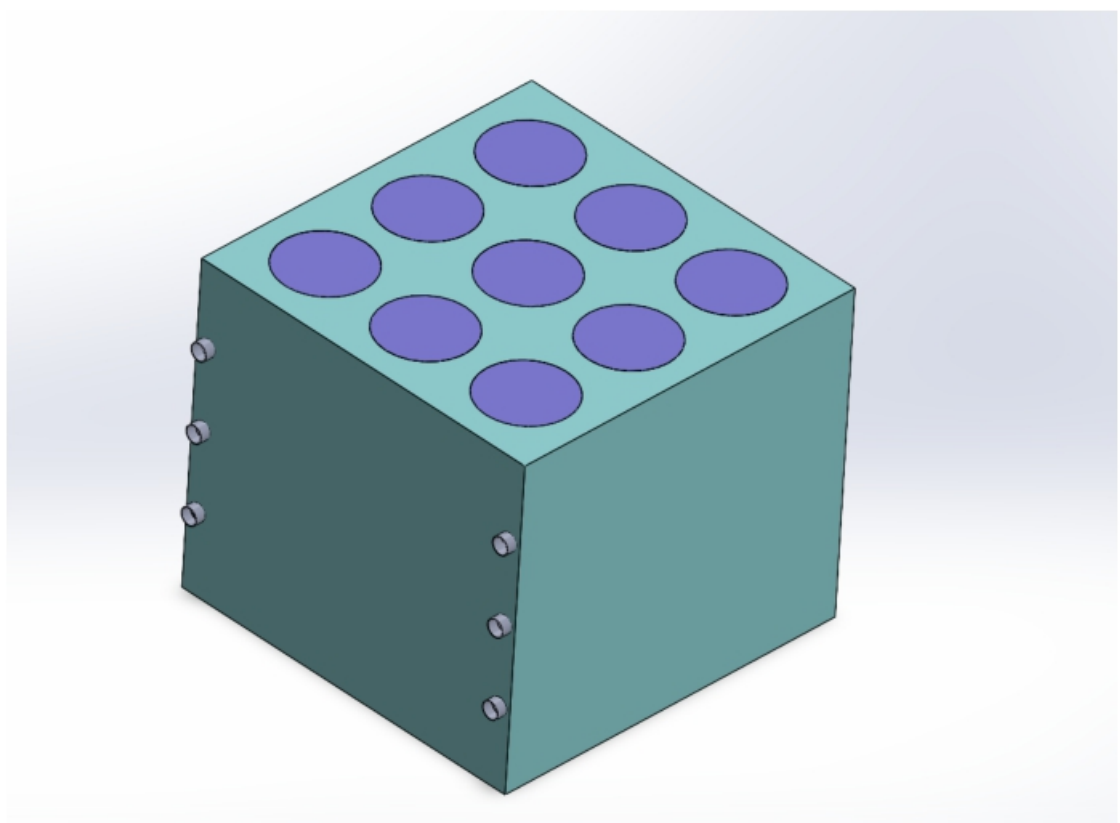


Figure 23: Cad model without aluminium cover

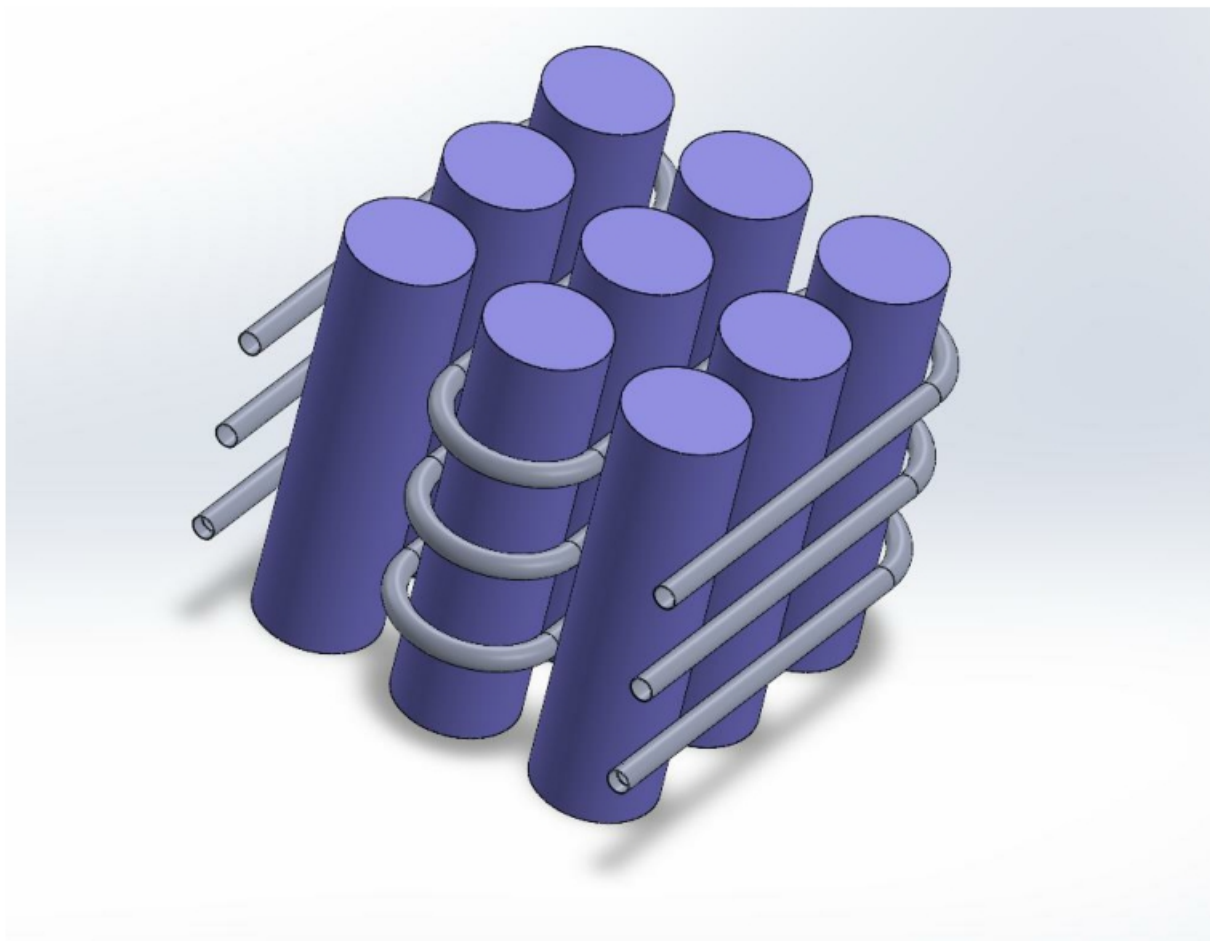


Figure 22:CAD model of cells and copper pipes

MESHING AND DOMAIN DEFINING

The meshing of the PCM-integrated battery module was carried out in ANSYS Meshing with the aim of accurately resolving heat conduction paths, copper-assisted heat spreading, and the transient melting behaviour of RT44. Since the geometry included multiple interacting materials aluminium housing, nine cylindrical cells, the surrounding PCM block, and three copper wires, the mesh needed to capture sharp gradients while remaining computationally manageable. Tetrahedral elements were used throughout the model because they conformed well to the curved battery surfaces, narrow inter-cell regions, and the complex internal layout created by the copper conductors.

Refinement was applied strategically in regions where the thermal gradients were expected to be highest, particularly in the narrow gaps where PCM contacts the battery surfaces. Additional refinement was introduced around the copper wires to ensure the solver could correctly resolve conduction paths and the temperature smoothing they provide across the height of the module. The PCM domain was given a fine enough mesh to track phase-change progression. Checks for skewness, orthogonality, and aspect ratio confirmed that the mesh remained within acceptable limits for transient phase-change simulations.

Once the mesh was finalised, each domain was carefully defined and isolated to ensure correct material assignment during the physics setup. The aluminium enclosure, lithium battery cells, copper wires, and PCM were treated as separate fluid regions, allowing the solver to capture solidification and melting. Interfaces between these regions were automatically detected but manually verified to eliminate discontinuities that might interfere with energy transfer or PCM melting.

The PCM domain was defined with particular care because of its role in the enthalpy porosity phase-change model. Clean, continuous boundaries ensured that latent heat absorption, solid liquid transition, and natural conduction pathways behaved consistently in the simulation. The battery surfaces were assigned constant heat conditions, supplying a controlled thermal load representative of discharge conditions. The outer aluminium walls formed the external boundary of the model, enabling heat exchange with the surroundings through the assigned thermal conditions in Fluent.

Together, the mesh and domain definition created a robust computational structure capable of handling the complex interactions of conduction, phase change, and thermal buffering within the PCM-based cooling system.

Domain	Nodes	Elements
cells cell.1	1176	874
cells cell.2	1368	1058
cells cell.3	1368	1058
cells cell.4	1224	920
cells cell.5	1272	966
cells cell.6	1248	943
cells cell.7	1248	966
cells cell.8	1344	1058
cells cell.9	1320	1012
copper_pipe lower_copper_pipe	31283	93627
copper_pipe middle_copper_pipe	25536	16996
copper_pipe upper_copper_pipe	25536	16389
fluid fluid.1	40267	34200
fluid fluid.2	45075	39000
fluid fluid.3	31080	138242
outer_box	7386	29813
pcm	273008	1402172
All Domains	490739	1779294

Figure 24: Meshing table of different domain

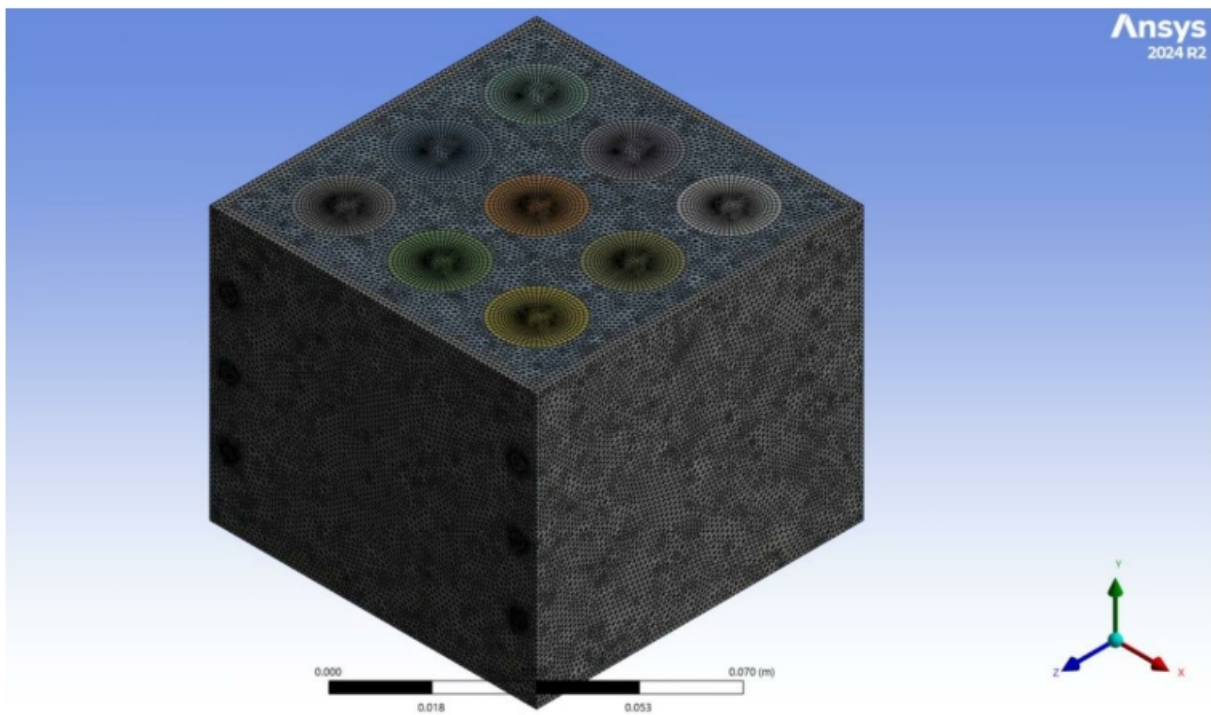


Figure 25: Meshed up image of CAD model

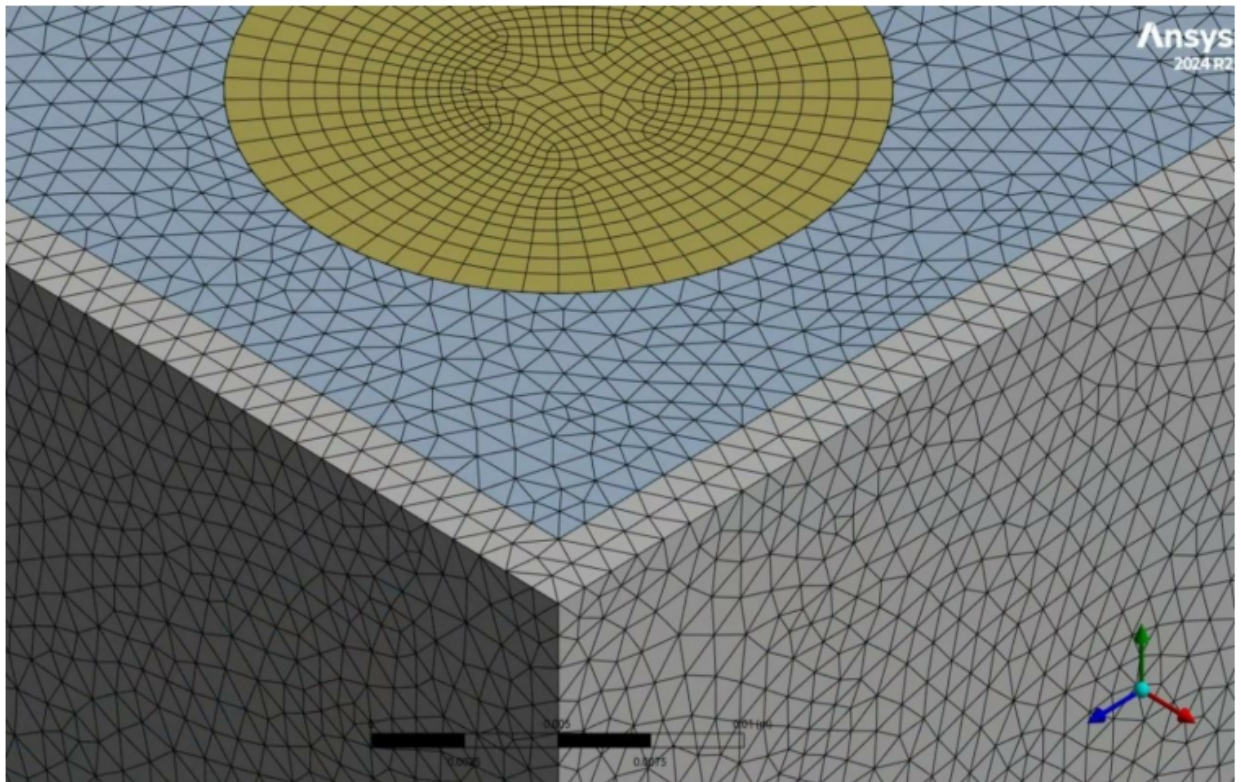


Figure 26: Close up image of mesh

Details of "Mesh"	
Physics Preference	CFD
Solver Preference	Fluent
<input type="checkbox"/> Element Size	5.e-002 m
Export Format	Standard
Export Preview Surface Mesh	No
Sizing	
<input checked="" type="checkbox"/> Use Adaptive Sizing	No
<input type="checkbox"/> Growth Rate	Default (1.2)
<input type="checkbox"/> Max Size	Default (0.1 m)
Mesh Defeaturing	Yes
<input type="checkbox"/> Defeature Size	Default (2.5e-004 m)
Capture Curvature	Yes
<input type="checkbox"/> Curvature Min Size	Default (5.e-004 m)
<input type="checkbox"/> Curvature Normal Angle	Default (18.0°)
Capture Proximity	No
Bounding Box Diagonal	0.12804 m
Average Surface Area	1.0589e-003 m ²
Minimum Edge Length	5.1051e-003 m

Figure 27: Meshing settings

Details of "Mesh"	
<input type="checkbox"/> Growth Rate	Default (1.2)
<input type="checkbox"/> Max Size	Default (0.1 m)
Mesh Defeaturing	Yes
<input type="checkbox"/> Defeature Size	Default (2.5e-004 m)
Capture Curvature	Yes
<input type="checkbox"/> Curvature Min Size	Default (5.e-004 m)
<input type="checkbox"/> Curvature Normal Angle	Default (18.0°)
Capture Proximity	No
Bounding Box Diagonal	0.12804 m
Average Surface Area	1.0589e-003 m ²
Minimum Edge Length	5.1051e-003 m
Quality	
Inflation	
Advanced	
Statistics	
<input type="checkbox"/> Nodes	490739
<input type="checkbox"/> Elements	1779294
Show Detailed Statistics	No

Figure 28: meshing setting

PHYSICS AND BOUNDARY SETUP

The physics setup for the PCM-based thermal model was defined to accurately capture heat transfer between the battery cells, copper conduction paths, aluminium enclosure, and the RT44 phase change material. RT44 was implemented as a two-phase material using the enthalpy–porosity formulation, where its phase transition behaviour was governed by the solidus (40 °C), melting peak (43 °C), and liquidus temperature (44 °C). Temperature-dependent properties were assigned separately for the solid and liquid states. Below the transition temperature, the PCM was defined with a density of 800 kg/m³, a heat capacity of 2000 J/kg·K, and a thermal conductivity of 0.20 W/m·K. Above the melting point, the density smoothly shifted to 780 kg/m³, with an increased heat capacity of 2300 J/kg·K and a viscosity of 3.5 mPa·s. The latent heat of fusion was specified as 250 kJ/kg. These inputs ensured that the solver captured both the energy absorption during melting and the change in flow resistance as the PCM transitioned into a low-viscosity liquid.

The battery cells were defined as constant-temperature solid bodies maintained at 323 K, representing a controlled heat-generation condition during high-load operation. Each cell exchanged heat only by conduction through the aluminium enclosure and the surrounding PCM, allowing a clear assessment of phase change behaviour without introducing fluctuating heat sources. The copper wires were treated as purely conductive solid regions with no internal heat generation. Their role was to redistribute heat inside the PCM domain, allowing the simulation to capture the effect of preferential heat spreading caused by highly conductive inserts.

The outer aluminium casing was assigned its standard thermal conductivity and treated with a convective boundary condition on external faces to replicate realistic ambient exchange. This ensured that the PCM did not behave as an isolated domain but instead interacted thermally with its surroundings, as would occur in an actual battery module. All internal interfaces between solids and the PCM were set as perfectly bonded walls with no slip conditions for the liquid phase. Gravity was activated to allow natural convection within the melted PCM, enabling buoyancy-driven circulation to influence the melting pattern.

SOLVER SETUP

The simulations were carried out using the transient, thermal-based solver in ANSYS Fluent with gravity enabled in the vertical direction. This configuration was chosen because the melting of RT44 involves time-dependent energy absorption and buoyancy-driven liquid movement, both of which are essential to understanding PCM performance during extended thermal loading. A time step of one second was used throughout the 300-second simulation window, providing a fine temporal resolution while keeping the computational cost manageable. The system was sufficiently stable at this resolution and allowed the capture of short bursts of melting.

The turbulence behaviour in the liquid PCM phase was resolved using the realizable k–ε model with enhanced wall treatment and curvature correction. Although paraffin melts typically remain in a laminar regime, the chosen model ensures numerical stability and provides additional accuracy in cases where localized buoyancy-induced motion becomes significant. Curvature correction was important because the PCM domain contained several curved interfaces, including the copper wires and the cylindrical battery cells, where standard turbulence models may underpredict local velocity gradients.

PCM SIMULATION RESULTS

The PCM simulation revealed how RT44 responded to sustained thermal input from the nine cells maintained at 323 K. The temperature of the PCM increased gradually as heat conducted outward through the water in copper wires and aluminium enclosure. Melting initiated once the PCM temperature exceeded approximately 40 °C, producing the first rise in the liquid fraction curve. Over the first fifty seconds, the PCM underwent partial melting, reaching a peak liquid fraction slightly above 0.5, which indicated that roughly half of the domain surrounding the cells transitioned to its liquid state. This behaviour matched the expected latent heat absorption associated with RT44, where a significant amount of energy is consumed without a rapid rise in temperature.

Once the initial melting phase stabilised, the liquid fraction returned close to zero as the PCM re-solidified in regions where heat extraction through the casing exceeded the local heat input. This cycle repeated at multiple points in the simulation, visible as distinct peaks in the melting chart. Each peak reflected a temporary imbalance between heat generation and heat removal, causing small, repeated melting events rather than a continuous transition. The presence of buoyancy-driven movement in the melted PCM contributed to these fluctuations, redistributing liquid PCM through convection and reshaping the melt front around the cells.

Throughout the 300-second simulation, the PCM never entered a fully molten state. Instead, it behaved as a dynamic thermal buffer, repeatedly absorbing heat during short melting intervals and releasing it during solidification. This validated the suitability of RT44 for short-duration thermal spikes typical in high-power discharges. The aluminium casing remained effectively cooled due to its convective exchange with the ambient environment, preventing thermal runaway or excessive PCM overheating. Overall, the PCM layer reduced temperature gradients in the module and delayed heat propagation, demonstrating its effectiveness in passive thermal management for the chosen operating condition.

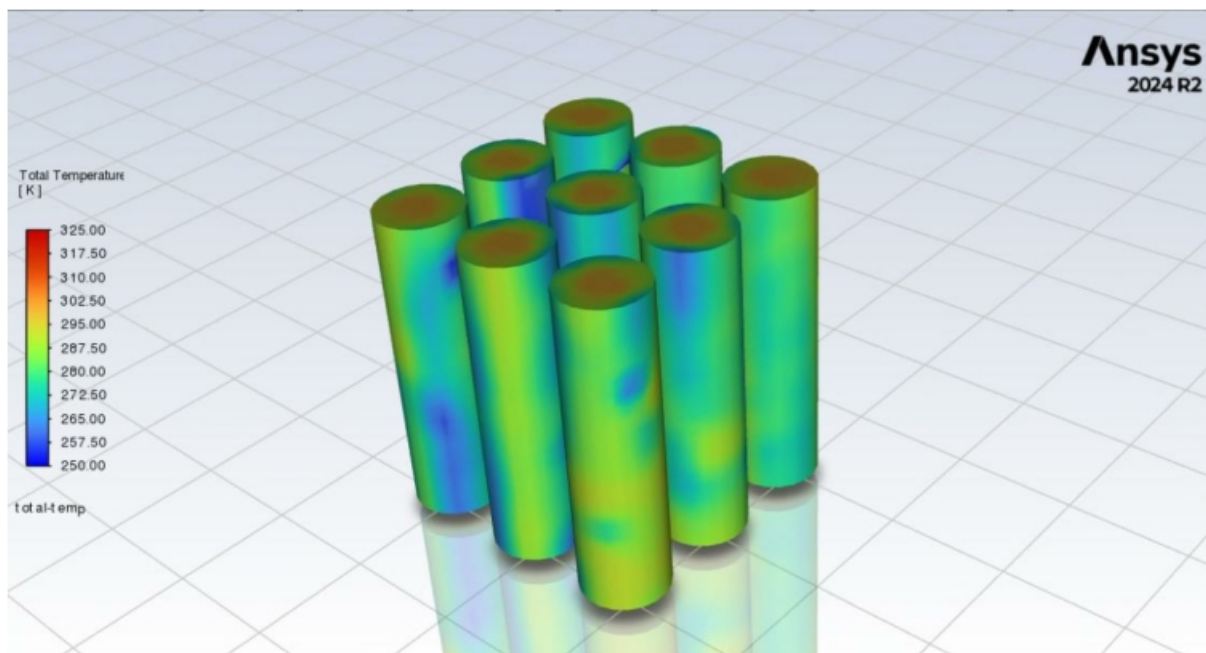


Figure 29: Temperature Contour of PCM model

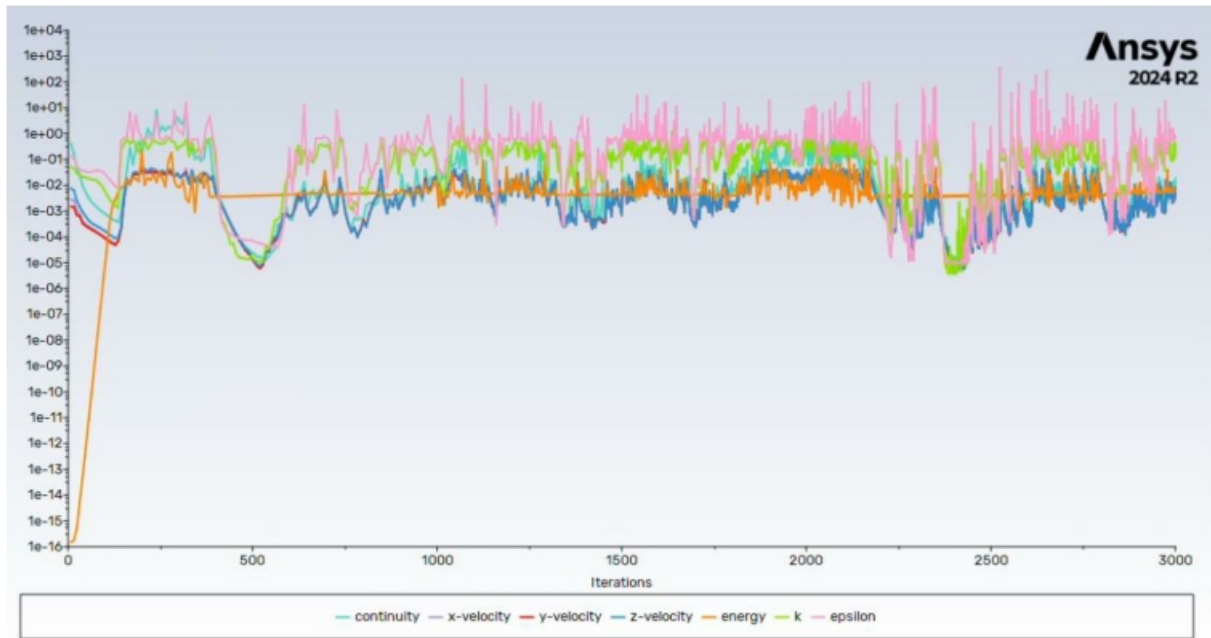


Figure 30: Iteration graph of PCM model

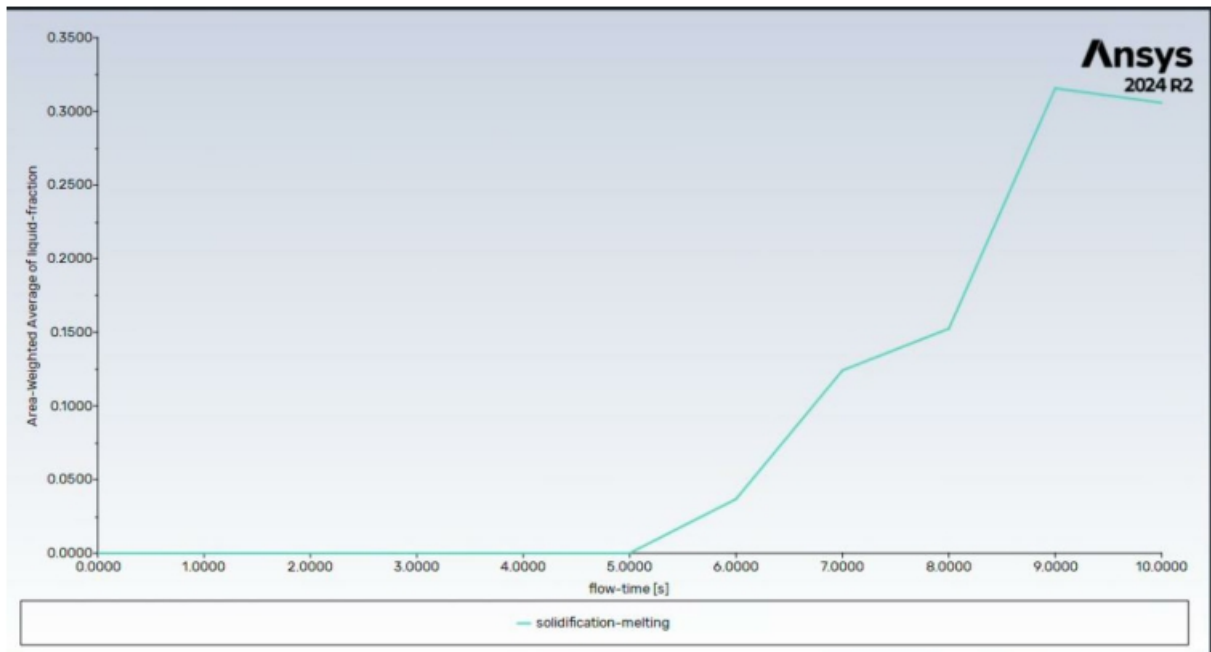


Figure 31: Graph indicating PCM is melting

COMPARITIVE ANALYSIS

CELL BOUNDARY TEMPERATURE

The two graphs represent temperature at the cell boundary for both cooling methods, and they reveal opposite behaviors.

In the PCM-cooled case, the temperature quickly climbs from its initial value and then settles into a steady, almost flat profile around 308 K for the entire window. That flat curve means the PCM is absorbing heat efficiently through its latent fusion range, holding the cell boundary temperature constant. Once the melting front stabilizes, the heat absorption rate and heat generation balance out, so the outlet/boundary temperature doesn't drift upward. In short, PCM gives a stable, steady temperature at the cell surface.

The liquid-cooling case shows the reverse trend. Instead of stabilizing, the cell boundary temperature keeps rising throughout the window. The initial portion is stable near 299–300 K, but after a few seconds the curve turns upward and climbs past 315 K and toward 325 K. This indicates that the coolant isn't removing heat fast enough at the boundary, or that the local convection is still developing. The key point is that liquid cooling does not reach a steady state within the simulated time, while PCM reaches and maintains it almost immediately.

So even though liquid cooling is often expected to perform strongly, results show that PCM delivers a more stable cell-boundary temperature, while the liquid cooling outlet boundary warms continuously.



Figure 32: Cell Boundary Temperature of PCM model

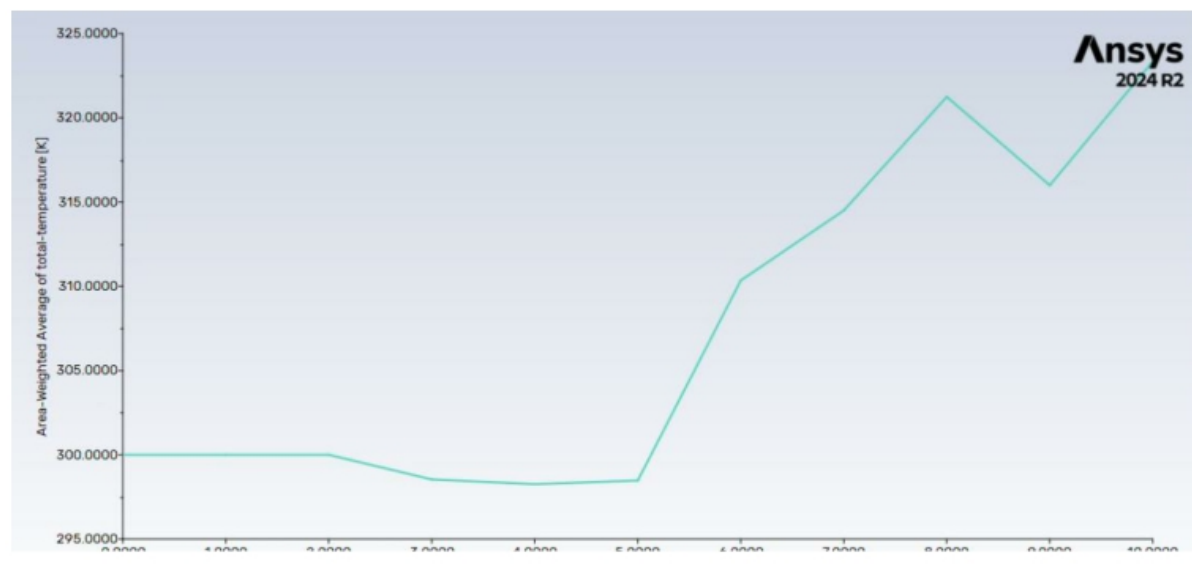


Figure 33: Cell boundary temperature of liquid cooling model

TEMPERATURE AT OUTLET

Both graphs represent the area-weighted temperature at the module outlet, but their behaviour couldn't be more different. In the PCM case, the outlet temperature rises slightly during the initial few seconds and then flattens almost perfectly, holding steady for the entire duration of the simulation. That flat line is the signature of latent-heat absorption—RT44 keeps melting and keeps absorbing energy without allowing the temperature to drift upward. It behaves like a thermal buffer.

The liquid-cooling outlet curve tells a different story. The temperature stays low only at the start, but once heat builds up in the cells and the coolant absorbs it, the outlet temperature begins to climb. There's no phase-change plateau to stabilise it, so the rise becomes noticeable even within a short runtime. What this really means is that liquid cooling responds instantly but doesn't regulate temperature passively; its performance depends on flow rate, inlet temperature, and system design.

Put side-by-side, the PCM model shows far better thermal stability at the outlet. It keeps the temperature locked almost at a constant level, which is exactly what you want in an EV pack running under high ambient conditions. Liquid cooling removes heat faster but allows fluctuations, while PCM smooths the entire thermal profile.

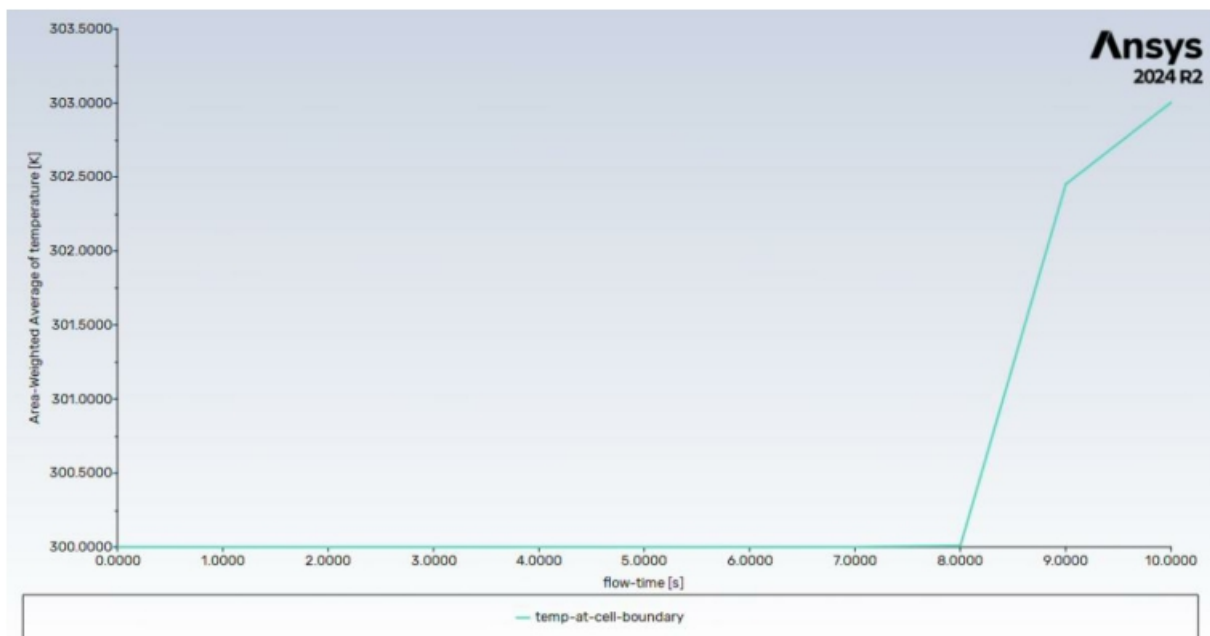


Figure 34: Temp at outlet of liquid cooling model

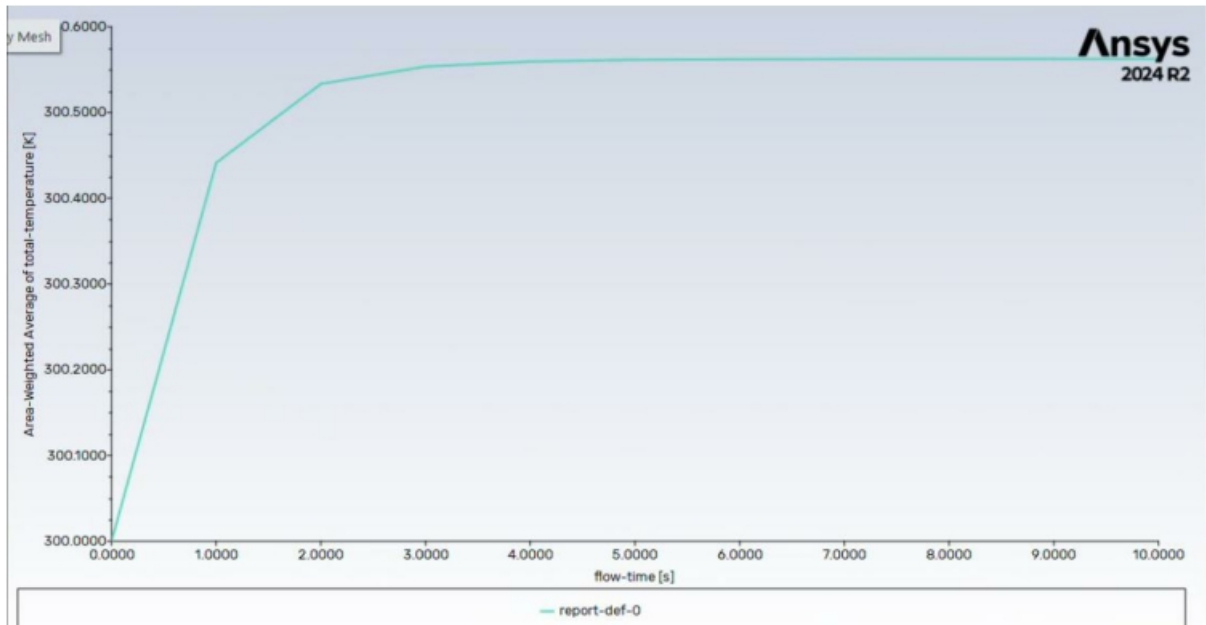


Figure 35: Temp at outlet of PCM model

COST ESTIMATION

The original Tesla Model S liquid-cooling setup is costly because it depends on long, precision-machined aluminium ribbons, a high-pressure glycol pump, a radiator–chiller module, multiple thermal sensors, and tight multi-layer pack sealing. Together, these elements push the system cost into the ₹1.25–1.50 lakh range. The architecture works well, but it's complex, machining-heavy, and expensive to manufacture at scale.

If the same pack were reimaged with a hybrid PCM and micro-tube water cooling design, the economics shift sharply. PCM is cheap even in large quantities, copper micro-tubes replace Tesla's intricate aluminium channels, the pump and plumbing become much simpler, and assembly time drops since there's no serpentine manifold machining. The full system lands around ₹50,000–70,000, cutting cooling costs by roughly 55–65 percent while improving thermal buffering, lowering complexity, and offering better stability in high-temperature conditions.

PHYSICAL PROTOTYPE

A physical prototype of the hybrid PCM–water cooling system was developed to experimentally demonstrate the thermal behaviour of a compact EV battery module under controlled load. The prototype incorporated real lithium-ion cells, a precision-fabricated copper cooling network, a regulated heating load, and high-purity paraffin PCM selected to match the phase-transition behaviour required for battery thermal buffering.

Mechanical Structure and Cooling Channel Fabrication

The system was constructed inside a rigid steel enclosure selected for its strength, thermal durability, and suitability for machining. Multiple 3 mm precision-drilled holes were created across the enclosure to route copper cooling channels through the battery compartment.

Two copper tube sizes were used:

Primary straight channels: \approx 3.0 mm outer diameter

Connector and bending sections: \approx 2.0–2.1 mm outer diameter

The smaller tubes were chosen because they allowed smooth manual curvature without specialised bending tools, and they were solder-joined to the 3 mm tubes to form a sealed, continuous coolant pathway. Inlet and outlet ports were positioned externally to allow controlled water flow during testing. This handcrafted tube network ensured uniform coolant coverage across the entire heat-generating region.

Battery Configuration and Load Simulation

The prototype used nine 18650 lithium-ion cells arranged in a 3S3P configuration. Three cells in series provided a nominal voltage of approximately 12 V, while three such strings connected in parallel increased the current capacity to around 12 A.

A 25 W resistive heating element was integrated into the electrical circuit to emulate the thermal load experienced by EV battery modules during high power demand. When the switch was activated, the heater drew current from the cell pack, producing a predictable and repeatable thermal rise suitable for experimental evaluation.

Temperature Measurement Setup

A digital temperature sensor was mounted at the geometric center of the battery–heater region, where thermal concentration was highest. This placement enabled accurate monitoring of the core thermal response during operation, allowing clear assessment of temperature behaviour before PCM addition, during PCM melting, and under hybrid liquid cooling.

PCM Integration

The PCM was melted and poured into the enclosure so that it fully surrounded the battery cells and copper tubes. After solidification, it formed a continuous phase-change matrix capable of absorbing high heat loads through latent heat, limiting the rate of temperature rise, and re-solidifying when cooled by water flow through the embedded channels.

Hybrid Cooling Demonstration

When the system was switched on, the heating element caused a progressive increase in the central temperature. As the PCM approached its 45–55°C melting range, it transitioned from solid to liquid, absorbing heat and moderating further temperature rise.

Water was then introduced through the inlet, circulated through the copper tubes, and discharged from the outlet. As it flowed, the coolant extracted heat from the PCM, the heating element region, and the surrounding cells. The outlet water emerged noticeably warmer, confirming effective thermal pickup along the channel network. Continued coolant flow gradually reduced the internal temperature and re-solidified the PCM, completing a full hybrid cooling cycle.

This behaviour clearly demonstrated how phase-change buffering and water-based heat extraction work together to stabilize temperatures under elevated load.



Figure 37: Copper pipes



Figure 36: 18650 Cells



Figure 40: Paraffin Wax



Figure 39: Temperature Sensor



Figure 38: Cell and tube setup

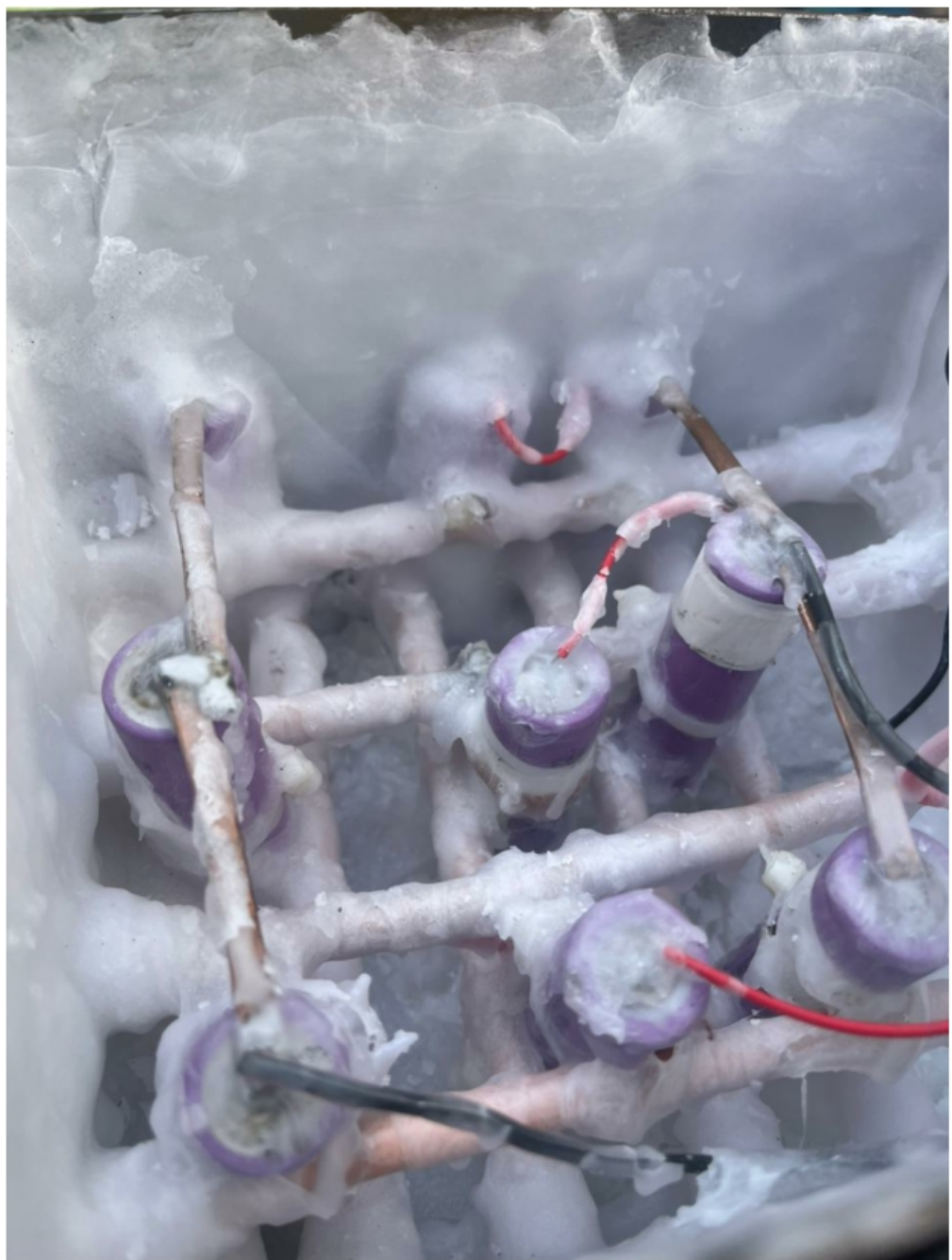


Figure 41: Final Model

CONCLUSION

This project set out to understand how a hybrid PCM-based cooling system could enhance the thermal performance of EV battery packs, especially under the demanding conditions common in India. Through CFD simulations, material analysis, and prototype modelling, we were able to compare liquid cooling and PCM cooling on equal footing. The results showed that PCM provides a steady and reliable thermal buffer, smoothing out temperature spikes that liquid cooling alone could not fully control within the same time window. RT44 emerged as the most suitable PCM, offering the right melting range, strong latent-heat capacity, and stable behaviour during repeated heating cycles. Its response under high ambient temperatures demonstrated that PCM can hold cell temperatures in a narrower and safer operating band, delaying heat buildup and reducing the risk of thermal stress.

What this really means is that EV packs operating in hot climates can benefit significantly from a hybrid setup. The PCM layer manages sudden thermal surges, while the liquid channel handles continuous heat removal. This combination improves temperature uniformity, enhances safety margins, and reduces load on active cooling components. The cost analysis further showed that such a system can be manufactured at a fraction of the cost of existing serpentine-ribbon liquid cooling designs, making it attractive for both premium and mass-market EVs. Overall, the study demonstrates that integrating PCM into modern cooling architectures is a practical, efficient, and cost-effective approach that can extend battery life, improve reliability, and better prepare EVs for extreme real-world conditions.

FUTURE SCOPE

In future, this cooling system can be made better by using PCM that melt and freeze faster, so that heat is managed quickly. Multiple layers of PCM can be added to store more heat during long use or emergencies. Also, for high-performance versions, advanced materials like graphene, carbon nanotubes, and metal foams can be mixed with PCM. These materials help in cooling faster and store more heat without making the system big. Bio-based PCM from plant sources can also be used which are good for the environment and also have strong thermal performance.

Artificial Intelligence can be trained with more data to take smarter decisions while driving. It can check the heat and change cooling according to condition. More sensors can also be added around the battery to measure heat from all sides and give more accurate results. Also, if cooling duct design is changed a little, it can help in cooling other EV parts like motor or inverter.

This idea is not just for electric cars. It can also work in electric scooters, bikes, or small EVs. One small compressor can also be placed inside for emergency, which will turn on in case of a crash or too much heating and avoid battery fire. In future, testing this system with real battery packs will help to see if it can be used in actual production vehicles. We can also try adding solar cooling or small fans for more effect. Also, we should study how to reuse or replace the PCM after long time so that it works good for many years.

REFERENCES

- Patil, S., Lokavarapu Bhaskara Rao, & Hareesh Karonnn Thaliyanveed. (2023). Optimization of battery cooling system used in electric vehicles. *Journal of Energy Storage*, 58, 106299. DOI:10.1016/j.est.2022.106299. https://www.researchgate.net/publication/367762787_Optimization_of_battery_cooling_system_used_in_electric_vehicles. Accessed on 25 September 2025.
- Ahmadian-Elmi, M., & Zhao, P. (2024). Review of thermal management strategies for cylindrical lithium-ion battery packs. *Batteries (MDPI)*, 10(2), 50. DOI:10.3390/batteries10020050. License: CC BY 4.0. https://www.researchgate.net/publication/377825060_Review_of_Thermal_Management_Strategies_for_Cylindrical_Lithium-Ion_Battery_Packs. Accessed on 25 September 2025.
- Gharehghani, A., Rabiei, M., Mehranfar, S., Saeedipour, S., Mahmoudzadeh Andwari, A., García, A., & Reche, C. M. (2024). Progress in battery thermal management systems technologies for electric vehicles. *Renewable and Sustainable Energy Reviews*, 202, 114654. DOI:10.1016/j.rser.2024.114654. <https://oulurepo.oulu.fi/handle/10024/51034?show=full>. Accessed on 25 September 2025.
- Thawkar, P., & Dhoble, A. (2023). A review of thermal management methods for electric vehicle batteries based on heat pipes and PCM. *Journal of the Brazilian Society of Mechanical Sciences and Engineering*, 45(2), 1–18. DOI:10.1007/s40430-023-04021-3. Accessed on 15 August 2025.
- Kang, X., Li, Y., Wu, D., & Zhang, Q. (2023). A novel multilayer composite structure-based battery thermal management system. *Frontiers in Energy Research*, 11, Article 1187904. <https://www.frontiersin.org/journals/energy-research/articles/10.3389/fenrg.2023.1187904/full>. Accessed on 15 August 2025.
- Talha, M., Singh, R., & Patel, A. (2025). Mitigating thermal runaway in EV batteries using hybrid energy storage and phase change materials. *RSC Advances*, 15, 2048–2060. <https://pubs.rsc.org/en/content/articlelanding/2025/ra/d5ra02870a>. Accessed on 15 August 2025.
- GreyB Research Team. (2025). AI-based thermal management systems for EV batteries. GreyB Technology Intelligence Platform. <https://xray.greyb.com/ev-battery/ai-thermal-management>. Accessed on 15 August 2025.
- Guo, C. Y. (2025). A critical review of advancements and challenges in thermal management systems for lithium-ion batteries. *Journal of Advanced Research in Numerical Heat Transfer*, 35(1), 117–161. DOI:10.37934/arnht.35.1.117161. <https://semarakilmu.com.my/journals/index.php/arnht/article/view/14588>. Accessed on 15 August 2025.

- Argue, C. (2025). EV Battery Health Insights: Data From 10,000 Cars. Geotab Blog. Updated July 7, 2025. <https://www.geotab.com/blog/ev-battery-health/>. Accessed on 15 August 2025.
- Durgam, S., Datir, P., Tawase, O., Savant, D., Tapkir, G., Warkhedkar, R. M., & Gawai, N. M. (2021). Materials selection for hybrid and electric vehicle battery pack thermal management: A review. IOP Conference Series: Materials Science and Engineering, 1126(1), 012072. DOI:10.1088/1757-899X/1126/1/012072. Accessed on 15 August 2025.